

# On the root mean square error (RMSE) calculation for parameter estimation of photovoltaic models: A novel exact analytical solution based on Lambert $W$ function

Martin Čalasan<sup>a</sup>, Shady H. E. Abdel Aleem<sup>b</sup>, Ahmed F. Zobaa<sup>c,\*</sup>

<sup>a</sup> Faculty of Electrical Engineering, University of Montenegro, Montenegro

<sup>b</sup> 15<sup>th</sup> of May Higher Institute of Engineering, Mathematical and Physical Sciences, Cairo, Egypt

<sup>c</sup> College of Engineering, Design & Physical Sciences, Brunel University London, Uxbridge United Kingdom

\*Corresponding author

E-mail addresses: [martinc@ucg.ac.me](mailto:martinc@ucg.ac.me) (M. Čalasan), [engyshady@ieee.org](mailto:engyshady@ieee.org) (S. Abdel Aleem), and [azobaa@ieee.org](mailto:azobaa@ieee.org) (A. Zobaa).

1 **Abstract**

2 In the literature, one can find a lot of methods and techniques employed to estimate single diode solar  
3 photovoltaic (PV) cell parameters. The efficiency of these methods is usually tested by calculating the  
4 Root Mean Square Error (RMSE) between the measured and estimated values of the solar PV cell output  
5 current. In this work, first, the values of RMSE calculated using 69 different methods published in many  
6 journal papers for the well-known RTC France solar PV cell are presented and discussed. Second, a novel  
7 exact analytical solution for RMSE calculation based on the Lambert  $W$  function is proposed. The results  
8 obtained show that the RMSE values were not calculated correctly in most of the methods presented in  
9 the literature since the exact expression of the calculated cell output current was not used. Third, the  
10 precision of calculation of the methods used for analytical solving of Lambert  $W$  equation is presented  
11 and discussed. Fourth, the applicability of the proposed solution methodology in accordance with current-  
12 voltage characteristics measured in the laboratory for solar modules of Clean Energy Trainer Setup is  
13 checked. Identification of its unknown parameters is presented using three optimization techniques.  
14 Further, the proposed solution methodology is proven for Solarex MSX-60 PV module, and the most  
15 promising 5-parameter single diode parameters are estimated based on minimization of the precise  
16 RMSE values calculated. Finally, this work aimed to develop a good base for proper investigation and  
17 implementation of optimization algorithms to solve the parameter estimation problem of 5-parameter  
18 single diode PV equivalent circuits.

19

20 **Keywords**—Lambert  $W$  function; optimization; PV parameter estimation; root mean square error; RTC  
21 France solar cell; 5-parameter single diode model.

## 22 Abbreviations

23	ABC	Artificial bee colony
24	ABSO	Artificial bee swarm optimization
25	ABCDE	Artificial bee colony-differential evolution
26	A&I	Analytical and iterative based methods
27	BPFPA	Bee pollinator flower pollination algorithm
28	BMO	Bird mating optimizer
29	BBO	Biogeography-based optimization
30	BBO-M	Biogeography-based optimization algorithm with two mutation strategies
31	BC	Bézier curves
32	BHCS	Biogeography-based heterogeneous cuckoo search
33	CARO	Chaotic asexual reproduction optimization
34	COA	Chaotic optimization approach
35	CPMPSO	Classified perturbation mutation-based particle swarm optimization
36	CWOA	Chaotic whale optimization algorithm
37	CSO	Cat swarm optimization
38	DE	Differential evolution
39	DET	DE technique
40	EAs	Evolutionary algorithms
41	EHA-NMS	Eagle-based hybrid adaptive Nelder-Mead simplex algorithm
42	ER-WCA	Evaporation rate-based water cycle algorithm
43	FPSO	Flexible particle swarm optimization
44	FA	Firefly algorithm
45	FPA	Flower pollination algorithm
46	GGHS	Grouping-based global harmony search
47	GA	Genetic algorithm
48	GAMS	General algebraic modelling system
49	GOTLBO	Generalized oppositional teaching learning-based optimization
50	GWO	Grey wolf optimization
51	HFAPS	Hybrid firefly and pattern search algorithms
52	HS	Harmony search
53	HPEPD	High performing extraction procedure for the one-diode model
54	HISA	Hybridized interior search algorithm
55	HCLPSO	Chaotic heterogeneous comprehensive learning particle swarm optimizer
56	IADE	Improved adaptive DE
57	ICA	Imperialist competitive algorithm
58	ITLBO	Improved teaching-learning-based optimization
59	ISCE	Improved shuffled complex evolution
60	ILCOA	Improved Lozi map-based chaotic optimization algorithm
61	IGHS	Innovative global HS
62	IJAYA	Improved JAYA optimization algorithm
63	JAYA	Sanskrit word meaning victory or triumph
64	LI	Linear identification
65	LMSA	Levenberg-Marquardt algorithm combined with simulated annealing
66	MABC	Modified artificial bee colony algorithm
67	MADE	Memetic adaptive DE
68	MBA	Mine blast algorithm
69	MVO	Multi-verse optimization
70	MPCOA	Mutative-scale parallel chaos optimization algorithm
71	MPSO	Modified particle swarm optimization
72	MSSO	Modified simplified swarm optimization algorithm
73	NM	Newton method
74	NM-MPSO	Nelder-mead and modified particle swarm optimization
75	OBWOA	Opposition-based whale optimization algorithm
76	Rcr-IJADE	Rate crossover repairing improved adaptive DE
77	PCE	Population classification evolution
78	PS	Pattern search
79	PSO	Particle swarm optimization
80	PPSO	Parallel PSO
81	PGJAYA	Performance-guided JAYA algorithm
82	pSFS	Perturbed stochastic fractal search
83	PV	Photovoltaic

84	SA	Simulated annealing
85	SSE	Sum of squared error
86	STFT	Special trans function theory
87	TLBO	Teaching-learning-based optimization
88	TLABC	Teaching-learning-based artificial bee colony
89	TS	Taylor series
90	TVA-CPSO	Time-varying acceleration coefficients PSO
91	WCA	Water cycle algorithm
92	WDO	Wind-driven optimization

### 93 **Nomenclature**

94	$G$	Irradiance ( $\text{W}/\text{m}^2$ )
95	$I-U$	Current-voltage characteristics
96	$I_i^{meas}$ and $I_i^{calc}$	Measured and estimated solar cell current at point $i$ , respectively
97	$I_{pv}$	Photo-generated current
98	$I_0$	Reverse saturation current
99	$K_B$	Boltzmann constant
100	$M$	Positive integer
101	$n$	Ideality factor of the diode
102	$N$	The number of the measured points
103	$Pr$	Precision of calculation that reflects accuracy at higher values
104	$P-U$	Power-voltage characteristics
105	$Pr_{STFT}$ and $Pr_{Taylor}$	Precision of calculation using STFT and TS, respectively
106	$q$	Electron's charge
107	$RMSE$	Root mean square error
108	$R_P$	Parallel resistance of the solar cell
109	$R_S$	Series resistance of the solar cell
110	$T$	Actual temperature in Kelvin
111	$V_{th}$	Thermal voltage
112	$W$	Solution of the Lambert equation
113	$\beta$	Real number in Lambert W equation

## 114 1. Introduction

115 Recently, significant scaling up renewable energy sources (RESs) capacity in modern  
116 power systems is experienced in response to several technical, economic, environmental,  
117 social, and political factors. The conventional fossil fuel generation sources are facing severe  
118 environmental problems such as the greenhouse gas emissions contributing to global warming,  
119 and techno-economic problems due to price fluctuations and fuel depletion across the world  
120 [1,2]. In this regard, the solar photovoltaic (PV) capacity is one of the primary drivers towards  
121 realizing emission-free power generation that can accelerate shifting power systems away from  
122 fossil fuel generation sources to renewable sources.

123 Solar PV modules considerably depend on the operating conditions such as solar  
124 irradiance, temperature, spectrum, and others, particularly for PV modules installed outdoors.  
125 These particular PV modules have different electrical characteristics from the reference  
126 characteristics given in the manufacturer datasheets. What makes the problem more difficult is  
127 the incomplete data and missing parameters in the data sheets provided by the manufacturers  
128 and vendors. This is why it is not simple to model the nonlinear electrical characteristics  
129 precisely with the missing data. Besides, the need for accurate solar PV modules becomes  
130 crucial, particularly with the fast-growing solar PV capacity across the world. The practical  
131 realization of any solar PV system requires an adequate solar PV cell model as well as  
132 accurately determined solar cell parameters to design reliable power systems with solar systems  
133 efficiently. Thus, it becomes essential to estimate such parameters for a complete and precise  
134 solar PV model that can closely match the experimental measures under different operation  
135 conditions [3,4].

136 The parameter estimation problem of solar PV cells represents a trendy scientific field  
137 for researches working with power and energy systems. In the literature, one can find a lot of  
138 methods and techniques employed to estimate single diode solar PV cell parameters [3–64], in  
139 which three primary classes for estimating the single diode solar PV cell parameters can be  
140 categorized into analytical, numerical (deterministic and metaheuristic), and hybrid methods  
141 [3]. The analytical methods use the  $I-U$  (current-voltage) and  $P-U$  (power-voltage) data curve  
142 and the other information provided in the datasheet to formulate the mathematical estimation  
143 optimization problem. They are easy to implement and imply less computational effort.  
144 However, these methods require simplifications or approximations of the expressions used,  
145 which has a significant impact on the solution's accuracy. Besides, the selected initial points  
146 from the  $I-U$  curve may influence the accuracy of the solution obtained [3]. On one hand,  
147 numerical methods include iterative techniques such as Newton-Raphson, Levenberg-

148 Marquardt, and linear identification [3,42,45] to provide accurate solutions; however, they  
149 suffer from locally optimal in non-convex optimization problems, in addition to the time  
150 consumption when obtaining global solutions because their performance is highly dependent  
151 on the initial values provided by the programmer. On the other hand, numerical methods  
152 include evolutionary algorithms (EAs) or metaheuristics. EAs are based on a trajectory or  
153 population of individuals that interact between exploration and exploitation phases to create a  
154 search path that can avoid local optima and achieve global/near-global solutions. EAs are  
155 classified into several categories as bio-inspired based algorithms, swarm intelligence-based  
156 algorithms, physics and chemistry-based algorithms, and others. Despite the fact that EAs have  
157 shown better-estimated parameters of PV equivalent circuits in terms of computational  
158 efficiency and precision of solutions compared to the analytical and deterministic methods,  
159 their performance is highly dependent on proper adjustment of the control parameters. The  
160 most popular EAs used for parameter estimation of PV equivalent circuits are the bio-inspired  
161 algorithms, which mimic ideas, processes, or biological behaviors that take place in nature. The  
162 main representatives of this group are MADE [12], ISCE [20], BPFPA [25], DET [37], FPA  
163 [44], DE [46], IADE [54], Rcr-IJADE [57], and GA [60]. Also, swarming-based EAs are  
164 modeled to mimic swarming behaviors of birds, cats, bees, fish, or others. CPMP SO [4],  
165 HCLPSO [6], FPSO [7], MPSO [18], FA [22], MSSO [24], CSO [31], MABC [35], TVA-  
166 CPSO [38], PPSO [39], ABC [48], ABSO [53,55], BMO [52], and PSO [61], are the main  
167 representatives of these swarming-based algorithms. Similarly, physics and chemistry-based  
168 algorithms that mimic physical, chemical ideas or concepts are used for parameter estimation  
169 of PV equivalent circuits. The main representatives of this group are ER-WCA [23], WDO  
170 [27], WCA [38], GGHS [56], HS [56], IGHS [56], and SA [59]. Another set is that inspired by  
171 the teaching and learning process such as GOTLBO [30], STLBO [47], and TLBO [47,51], or  
172 that inspired by chaotic behaviors such as ILCOA [11], COA [13], CWOA [28], CARO [41],  
173 and MPCOA [50]. In the optimization process, the objective function, in most cases, is to  
174 minimize the sum of the squared difference between the experimentally measured solar PV cell  
175 output current and the calculated one of a specified number of data points. The third category,  
176 hybrid methods, combines analytical and numerical optimization methods to achieve global  
177 solutions associated with high computational efficiency and convergence speed towards  
178 finding the global solution. However, hybrid methods such as HISA [5], BHCS [16], HFAPS  
179 [19], TLABC [21], NM-MPSO [32], EHA-NMS [40], and ABCDE [55] are high complexity  
180 level algorithms.

181 In many of the mentioned papers, comparisons of these algorithms were presented in  
182 terms of many criteria such as convergence characteristics, computational efficiency,  
183 complexity, time per iteration, and so forth [14]. Unfortunately, we can find a case in a research  
184 paper claiming that algorithm X gives better results in comparison with results obtained by  
185 using algorithms Y or Z. However, in another research paper, we can find results obtained by  
186 using algorithm Z are better than the results obtained with algorithm X without any comments  
187 on algorithm Y [46–48,55–58] even if the algorithms are compared after many runs (e.g. above  
188 20). Besides, in a few recently published papers, we can also find different authors' discussion  
189 on the accuracy of the results obtained, and the root mean square error (RMSE) calculated with  
190 the measured and estimated values of the solar PV cell output current for the 5-parameter single  
191 diode model of solar cell [62–64]. It is clear that no method has been evidenced to be the most  
192 appropriate method in identifying the unknown parameters and no guarantee is observed for  
193 realizing global solutions of the different PV modules. This necessitates an assessment of the  
194 solutions provided by the different methods to solve the solar PV cell parameters extraction  
195 problem of the different PV modules.

196 In response to these discussions, in this work, first, the values of RMSE calculated using  
197 69 different methods published in many journal papers for the well-known RTC France solar  
198 PV cell are presented and discussed. The RTC France solar cell is used in this work as it is one  
199 of the most popular solar cells across the world, and is commonly used in many published  
200 papers to test algorithms. Second, a novel exact analytical solution for RMSE calculation based  
201 on the Lambert  $W$  function is proposed. The results obtained show the shortcomings many of  
202 the reported works made with the determination of their RMSE calculations for the equivalent  
203 circuit modeling approach under focus. Third, the precision of two numerical approaches to  
204 numerically solve the Lambert  $W$  function is addressed and discussed with: (i) one based on  
205 Taylor series; and (ii) the other based on Special Trans Function Theory. Fourth, the  
206 applicability of the proposed solution methodology in accordance with current-voltage  
207 characteristics measured in the laboratory for solar modules of Clean Energy Trainer Setup is  
208 checked. Identification of its unknown parameters is presented using three optimization  
209 techniques: chaotic optimization algorithm (COA), evaporation rate water cycle algorithm  
210 (ER-WCA), and harmony search (HS). Further, the proposed solution methodology is applied  
211 for Solarex MSX–60 PV module, and the most promising 5 parameters are estimated based on  
212 the minimization of the precise RMSE values calculated. Finally, this work aimed to present a  
213 good base for proper investigation and implementation of optimization algorithms to solve the  
214 5-parameter estimation problem of the single diode equivalent circuits of PVs.

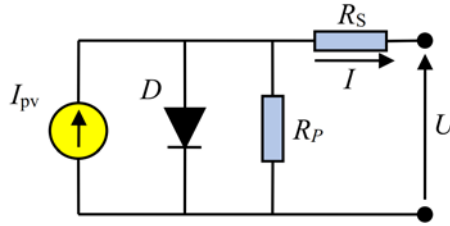
215 The rest of the work is organized as follows: In Section 2, a short description of the 5-  
 216 parameter single diode solar cell model is given. Also, the proposed RMSE expression based  
 217 on Lambert  $W$  function is presented. Values obtained of the proposed RMSE expression and  
 218 comparison of related works in the literature are presented and discussed in Section 3. Also,  
 219 the precision of two numerical approaches to numerically solve the Lambert  $W$  function is  
 220 addressed and discussed. In Section 4, the applicability of the proposed methodology is  
 221 presented with the aid of experimental results and optimization methods. Lastly, the concluding  
 222 remarks are drawn in Section 5.

223

## 224 2. Proposed RMSE calculation based on Lambert $W$ function

### 225 *Single diode solar cell model*

226 The single diode solar cell model is a commonly used model for solar cell representation [4].  
 227 This model consists of one current source, one diode, and two resistances, namely a series  
 228 resistance ( $R_S$ ) and a parallel resistance ( $R_P$ ), which represent the solar cell losses. The  
 229 equivalent circuit of the single diode PV cell model is shown in Fig. 1.



230

231

232

Fig. 1. Single diode model of the solar cell

233 In the mathematical sense, the  $I$ - $U$  relationship of this model can be described, as follows:

$$I = I_{pv} - I_0 \left( e^{\frac{U + IR_S}{n \times V_{th}}} - 1 \right) - \frac{U + IR_S}{R_p} \quad (1)$$

234 where  $I_{pv}$  represents the photo-generated current,  $I_0$  is the reverse saturation current,  $n$  is the  
 235 ideality factor of the diode, and  $V_{th} = K_B T / q$  is the thermal voltage ( $K_B$  is Boltzmann constant,  
 236  $T$  is the temperature and  $q$  is the electron's charge). In addition to the single-diode model, two-  
 237 diode and three-diode solar cell models can be found in the available literature [3]. However,  
 238 in regard to two-diode and three-diode solar cell models, no exact analytical solution has been  
 239 reached yet because of the high nonlinearity of the current expressions of these models.



240 *Conventional RMSE calculation*

241 In line with the literature [3-62], the following equation is usually expressed for the calculation  
 242 of RMSE between measured and calculated output current of the solar PV cell.

$$RMSE = \sqrt{\frac{1}{N} \sum_{i=1}^N (I_i^{meas} - I_i^{calc})^2} \quad (2)$$

243 where  $N$  represents the number of the measured points.  $I_i^{meas}$  and  $I_i^{calc}$  represent the measured  
 244 and estimated solar cell current at point  $i$ , respectively. Pseudo-substituting Eq. (1) into Eq. (2);  
 245 at  $U^{calc}=U^{meas}$ , one can formulate the RMSE expression as follows:

246

$$RMSE = \sqrt{\frac{1}{N} \sum_{i=1}^N \left( I_i^{meas} - \left( I_{pv} - I_0 \left( e^{\frac{U_i^{meas} + I_i^{meas} R_S}{n \times V_{th}}} - 1 \right) - \left( \frac{U_i^{meas} + I_i^{meas} R_S}{R_P} \right) \right) \right)^2} \quad (3)$$

247 However, with  $I_{PV} - I_0 \left( e^{\frac{U_i^{meas} + I_i^{meas} R_S}{n \times V_{th}}} - 1 \right) - \left( \frac{U_i^{meas} + I_i^{meas} R_S}{R_P} \right)$  in the general case, the last  
 248 part of this equation does not represent the calculated value of the solar cell output current, and  
 249 therefore, Eq. (3) is not a correct expression of the RMSE measure. It should be noted that  
 250 many reported works of the literature use this relation to estimate their RMSE.

251 *Lambert W function*

252 In mathematics, the Lambert  $W$  function is a set of functions, precisely the branches of  
 253 the inverse relation of the function  $\beta$  given below.

$$f(x) = \beta = xe^x \quad (4)$$

254 where  $e^x$  is the exponential function, and  $x$  is any complex number. Many problems in  
 255 engineering sciences can be described using this equation. Thus, one can get  $x$  as follows:

$$x = f^{-1}(xe^x) = W(\beta) \quad (5)$$

256 where  $W$  represents the solution of the Lambert equation [65-73]. A graphical representation  
 257 of the function  $\beta = xe^x$  is shown in Fig. 2.

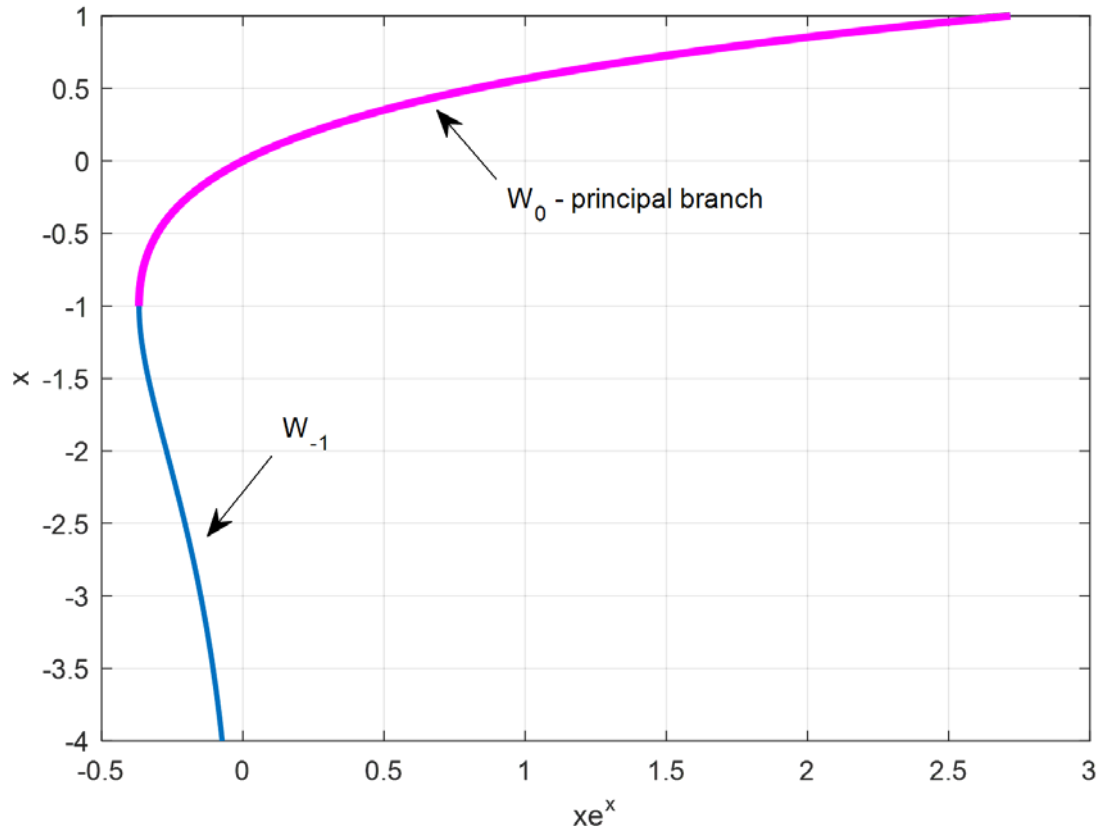


Fig. 2. Graphical representation of the function  $\beta = xe^x$

258

259 It can be noticed from Fig. 2 that the illustration consists of two parts; the upper part (branch)  
 260 with  $W \geq -1$  representing the function  $W_0$ , which is called the principal branch, and the lower  
 261 part (branch) with  $W \leq -1$  representing the function  $W_{-1}$ .

262 It should be noted that for solving Lambert W functions, different techniques can be used  
 263 such as the iterative methods [65] and program packages with corresponding solvers [66], in  
 264 addition to analytical-based methods such Taylor series (TS) [67] and Special Trans Function  
 265 Theory (STFT) [68–73].

266 The TS of  $W_0$  around 0 is based on the usage of the Lagrange inversion formula as  
 267 follows:

$$x = W(\beta) = \sum_{n=1}^{\infty} \frac{(-n)^{n-1}}{n!} \beta^n \quad (6)$$

268 In practice, Eq. (6) can be rewritten as follows:

$$x = W(\beta) = \sum_{n=1}^M \frac{(-n)^{n-1}}{n!} \beta^n \quad (7)$$

269 where M denotes a positive integer.

270 The Lambert W function can also be solved using STFT as follows:

$$x = \beta \frac{\sum_{n=0}^M \frac{\beta^n (M-n)^n}{n!}}{\sum_{n=0}^{M+1} \frac{\beta^n (M+1-n)^n}{n!}} \quad (8)$$

271 However, it should be noted that for the same value of positive integer  $M$ , the STFT gives  
 272 the much more accurate results. It should be noted that the accuracy of using these methods is  
 273 tested in many papers [66,68]. However, the general conclusion is that TS has good accuracy  
 274 for small values of  $\beta$ , which is not the case for the higher values of  $\beta$ . However, STFT methods  
 275 have a high level of accuracy for any value of  $\beta$ . To sum up, STFT is a more accurate method  
 276 for analytical solving of the Lambert  $W$  equation. The reader can refer to [66,68,72] to  
 277 find additional information and examples.

### 278 *Proposed RMSE calculation*

279 In order to calculate the estimated value of the solar cell output current, we need to solve  
 280 Eq. (1). However, Eq. (1) is a highly nonlinear equation, *i.e.*, transcendental equation. Thus; it  
 281 can be rearranged in the following form:

$$I = \frac{R_p (I_{pv} + I_0) - U}{R_s + R_p} - \frac{nV_{th}}{R_s} W(\beta) \quad (9)$$

282 So that

$$\beta = A \exp \left( \frac{R_p (R_s I_{pv} + R_s I_0 + U)}{nV_{th} (R_s + R_p)} \right) \quad (10)$$

$$A = \frac{I_0 R_p R_s}{nV_{th} (R_s + R_p)} \quad (11)$$

283 In Eq. (9),  $W$  represents the solution of the Lambert  $W$  function. In practice, for one value  
 284 of the solar cell voltage, we have a particular value of the solar cell current. Therefore, in the  
 285 calculation process, if we take a particular value of the solar cell voltage (equals to the  
 286 measured voltage value), we can calculate the solar cell current using Eq. (9). Thus, the  
 287 calculation of the proposed RMSE expression between measured and estimated solar cell  
 288 current can be realized in the following manner:

$$RMSE = \sqrt{\frac{1}{N} \sum_{i=1}^N \left( I_i^{meas} - \left( \frac{R_p (I_{pv} + I_0) - U_i^{meas}}{R_s + R_p} - \frac{nV_{th}}{R_s} W \left( A \exp \left( \frac{R_p (R_s I_{pv} + R_s I_0 + U_i^{meas})}{nV_{th} (R_s + R_p)} \right) \right) \right) \right)^2} \quad (12)$$

290 Equation (12) represents the analytical solution of the RMSE expression calculated  
 291 between the measured and estimated solar cell output current. Besides, the analytical solution  
 292 of the proposed RMSE expression using TS is expressed in the following form:

$$293 \quad RMSE = \sqrt{\frac{1}{N} \sum_{i=1}^N \left( I_i^{meas} - \left( \frac{R_P (I_{pv} + I_0) - U_i^{meas}}{R_S + R_P} - \frac{nV_{th}}{R_S} \cdot \sum_{n=1}^M \frac{(-n)^{n-1}}{n!} \left( A \exp \left( \frac{R_P (R_S I_{pv} + R_S I_0 + U_i^{meas})}{nV_{th} (R_S + R_P)} \right) \right)^n \right) \right)^2} \quad (13)$$

294 Also, the analytical solution of the proposed RMSE expression using STFT is expressed  
 295 as follows:

$$296 \quad RMSE = \sqrt{\frac{1}{N} \sum_{i=1}^N \left( I_i^{meas} - \frac{R_P (I_{pv} + I_0) - U_i^{meas}}{R_S + R_P} - \frac{nV_{th}}{R_S} \cdot \left( A \exp \left( \frac{R_P (R_S I_{pv} + R_S I_0 + U_i^{meas})}{nV_{th} (R_S + R_P)} \right) \right) \frac{\sum_{n=0}^M \left( \frac{A \exp \left( \frac{R_P (R_S I_{pv} + R_S I_0 + U_i^{meas})}{nV_{th} (R_S + R_P)} \right) \right)^n (M-n)^n}{n!}}{\sum_{n=0}^{M+1} \frac{\left( A \exp \left( \frac{R_P (R_S I_{pv} + R_S I_0 + U_i^{meas})}{nV_{th} (R_S + R_P)} \right) \right)^n (M+1-n)^n}{n!}} \right)^2} \quad (14)$$

297 As Lambert  $W$  function is very popular in science, many programming packages have  
 298 implemented a solver for solving Lambert  $W$  function. For example, in Matlab, we have a  
 299 function called *lambertw*. In Maple, it is simply called  $W$ , while in the *Mathematica* computer  
 300 algebra framework, the function is implemented under the name *ProductLog*.

### 301 3. Numerical results and discussion

302 In Table 1, for the well-known RTC France solar PV cell, the values of RMSE calculated  
 303 using 69 different methods reported in many journal papers are presented, which rely on the  
 304 same experimental current-voltage characteristics. **In the same table, the estimated values of**  
 305 **the 5 parameters are given. Besides, the RMSE values calculated using Eq. (3) and the corrected**  
 306 **RMSE values calculated using Eq. (12) are presented. It should be noted that the determination**  
 307 **of the 5 parameters is not addressed by the current methodology; however, many optimization**  
 308 **techniques rely on objective functions whose accuracy can be improved by the proposed RMSE**  
 309 **calculation.**

310 All the calculations were carried out into the Matlab program package, while the  
 311 computer simulations were carried out on a PC with Intel(R) Core (TM) i3-7020U CPU @ 2.30  
 312 GHz and 4 GB RAM. Accuracy of the solution of the Lambert  $W$  function was tested by using  
 313 the Lambert  $W$  equation embedded in Matlab, in which the accuracy was lower than  $10^{-16}$  for  
 314 all the points measured from the  $I-U$  characteristics. The central part of the Matlab code for

315 RMSE calculation based on the Lambert  $W$  function is given in Appendix 1. Also, a  
316 Mathematica code for solving the Lambert  $W$  equation is provided.

317 The procedure for RMSE calculation is summarized as follows:

318 For any measured point, we consider the voltage value and calculate the corresponding  
319 current using Eq. (9). We then apply Eq. (2) for all the points, thus giving Eq. (12). Eq. (12) is  
320 resolved in practice either by Eq. (13) or Eq. (14) numerical approaches (or both).

321 It can be seen from Table 1 that the differences between the calculated RMSE values and  
322 the RMSE values presented in the original papers are considerable. A graphical illustration of  
323 these differences, on a logarithmic scale, is shown in Fig. 3. We can find the same values of  
324 RMSE, as suggested in this work in just two papers [5,42] among 58. However, in [5,42], no  
325 comments were given about the exact analytical solution of RMSE calculation or the Lambert  
326  $W$  function. Also, looking at the data given in Table 1, it can be noticed that many authors had  
327 used Eq. (3) for RMSE calculation, which is only a rough approximation.

328 Besides, some researchers use a very compact number value (0.0264V) or a semi-  
329 compact number value as (0.02638V) of  $V_{th}$  instead of the long number formatting value, which  
330 also has a significant impact on the calculated RMSE value. The impact of  $V_{th}$  on the calculated  
331 RMSE value is shown in Fig. 4.

332 Apart from the wrong approach for RMSE calculation, the reasons for results  
333 mismatching of the minimum RMSE can also be:

- 334 • Authors do not use all measured points for RMSE calculation ( $N=26$ ),
- 335 • Complete dependence on heuristic optimization techniques to reach a better solution  
336 than the corresponding values reported in the literature. Each optimization technique  
337 may also have different complexity and/or parameters at different values from one  
338 paper to the other.
- 339 • Inaccurate solving of the Lambert  $W$  function.

340 However, with this analysis, we cannot conclude that algorithm X is the best, while  
341 algorithm Y is the worst. The cause lies in the fact that the authors should use the proposed  
342 straightforward RMSE equation during the solar cell parameters estimation process, which has  
343 a significant impact on the algorithm efficiency.

Table 1. Numerical results of the conventional and proposed RMSE for parameters estimation of the solar RTC France cell (Results with the minimum RMSE are given in bold)

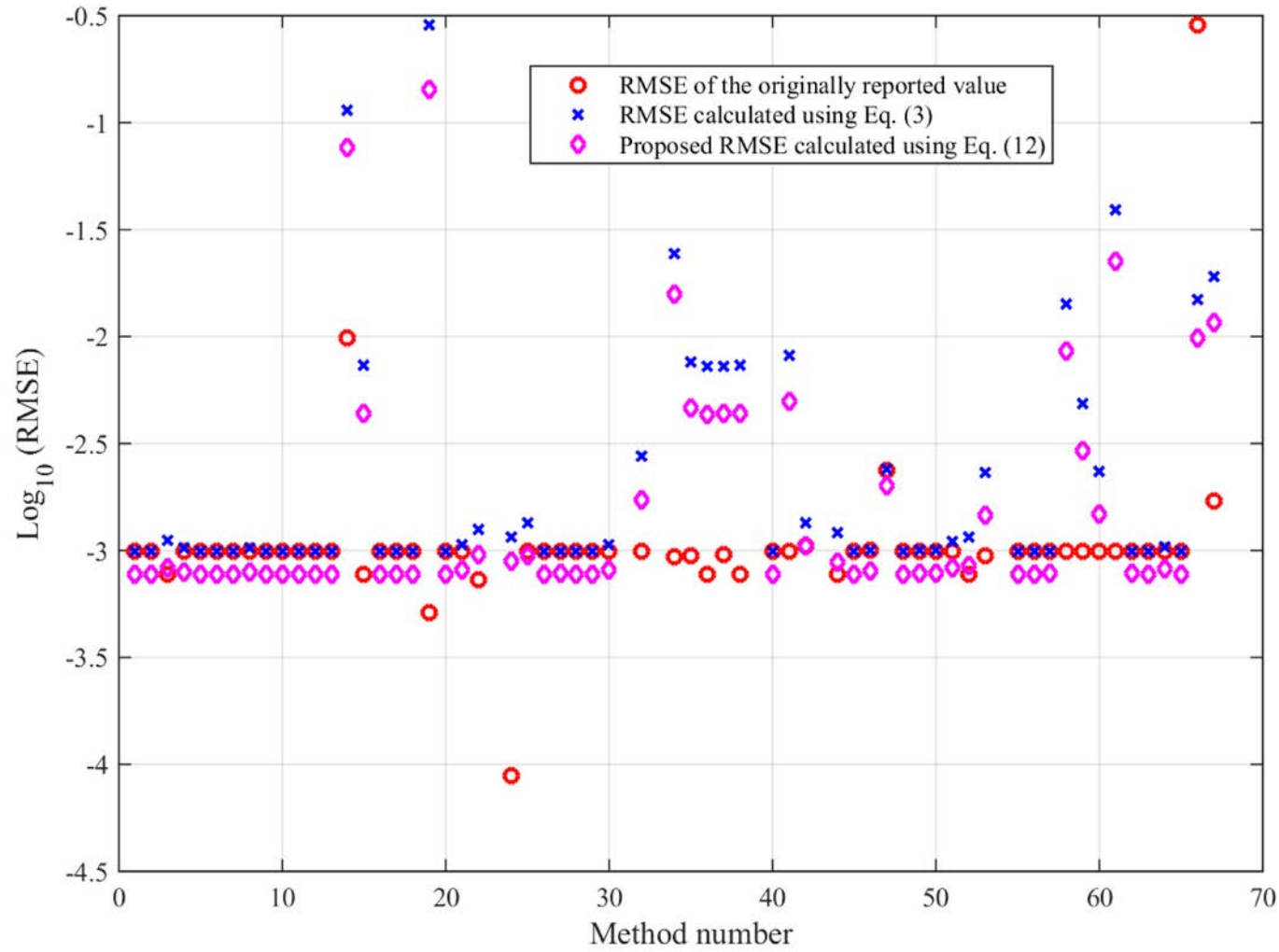
#	Ref.	Authors, year	Method	$I_{pv}$ (A)	$I_0$ ( $\mu$ A)	$n$	$R_s$ ( $\Omega$ )	$R_p$ ( $\Omega$ )	Original reported RMSE	RMSE calculated using Eq. (3)	Proposed RMSE calculated using Eq. (12)
1	[4]	Liang et al., 2020	CPMPSO	0.76077600	0.32302100	1.48118400	0.03637700	53.71852000	0.00098602	0.00098602	0.00077539
2	[5]	<b>Kler et al., 2019</b>	<b>HISA</b>	<b>0.76078797</b>	<b>0.31068459</b>	<b>1.47726778</b>	<b>0.03654695</b>	<b>52.88979426</b>	<b>0.00077301</b>	<b>0.00098911</b>	<b>0.00077301</b>
3	[6]	Dalia et al., 2019	HCLPSO	0.76079000	0.31062000	1.47710000	0.03654800	52.88500000	0.00077300	0.00112018	0.00083374
4	[7]	Ebrahimi et al., 2019	FPSO	0.76077552	0.32302000	1.48110817	0.03637000	53.71852000	0.00098602	0.00102203	0.00079112
5	[8]	Li et al., 2019	ITLBO	0.76080000	0.32300000	1.48120000	0.03640000	53.71850000	0.00098602	0.00099161	0.00077779
6	[9]	Chen et al., 2019	pSFS	0.76078000	0.32302000	1.48118000	0.03638000	53.71852000	0.00098602	0.00098608	0.00077542
7	[10]	Chen et al., 2019	ISCA	0.76077562	0.32301700	1.48118220	0.03637716	53.71821748	0.00098602	0.00098602	0.00077539
8	[11]	Pourmousa et al., 2019	ILCOA	0.76077500	0.32302100	1.48110800	0.03637700	53.71867900	0.00098602	0.00102229	0.00079167
9	[12]	Li et al., 2019	MADE	0.76080000	0.32300000	1.48120000	0.03640000	53.71850000	0.00098602	0.00099161	0.00077779
10	[13]	Calasan et al., 2019	COA	0.76077450	0.32300180	1.48117740	0.03637750	53.73000000	0.00098602	0.00098602	0.00077538
11	[14]	Yu et al., 2019	PGJAYA	0.76080000	0.32300000	1.48120000	0.03640000	53.71850000	0.00098602	0.00099161	0.00077779
12	[15]	Gnetchejo et al., 2019	GAMS	0.76077600	0.32302000	1.48118400	0.03637700	53.71852400	0.00098602	0.00098602	0.00077540
13	[16]	Chen et al., 2019	BHCS	0.76078000	0.32302000	1.48118000	0.03638000	53.71852000	0.00098602	0.00098608	0.00077542
14	[17]	Abd Elaziz et al., 2018	OBWOA	0.76077000	0.32320000	1.52080000	0.03630000	53.68360000	0.00098602	0.11416692	0.07674430
15	[18]	Manel et al., 2018	MPSO	0.76078700	0.31068300	1.47526200	0.03654600	52.88971000	0.00077301	0.00733027	0.00435991
16	[19]	Beigi et al., 2018	HFAPS	0.76077700	0.32262200	1.48106000	0.03638190	53.67840000	0.00098602	0.00098603	0.00077525
17	[20]	Gao et al., 2018	ISCE	0.76077553	0.32302083	1.48118360	0.03637709	53.71852771	0.00098602	0.00098602	0.00077539
18	[21]	Chen et al., 2018	TLABC	0.76078000	0.32302000	1.48118000	0.03638000	53.71636000	0.00098602	0.00098608	0.00077542
19	[22]	Louzazni et al., 2018	FA	0.76069712	0.43244110	1.45245666	0.03341059	53.40180803	0.00051382	0.28514264	0.14234113
20	[23]	Kler et al., 2017	ER-WCA	0.76077600	0.32269900	1.48108000	0.03638100	53.69100000	0.00098602	0.00098609	0.00077529
21	[24]	Lin et al., 2017	MSSO	0.76077700	0.32356400	1.48124400	0.03637000	53.74246500	0.00098607	0.00105990	0.00080916
22	[25]	Ram et al., 2017	BPFPA	0.76000000	0.31060000	1.47740000	0.03660000	57.71510000	0.00072700	0.00125359	0.00095551
23	[26]	Fathy et al., 2017	ICA	0.76030000	0.14650000	1.44210000	0.03890000	41.15770000	NG*	0.11581627	0.07502096
24	[27]	Derick et al., 2017	WDO	0.76080000	0.32230000	1.48080000	0.03676800	57.74614000	0.0008866	0.00115725	0.00089482
25	[28]	Oliva et al., 2017	CWOA	0.76077000	0.32390000	1.48120000	0.03636000	53.79870000	0.00098602	0.00134855	0.00094834
26	[29]	Yu et al., 2017	IJAYA	0.76080000	0.32280000	1.48110000	0.03640000	53.75950000	0.00098603	0.00098714	0.00077606
27	[30]	Chen et al., 2016	GOTLBO	0.76078000	0.33155200	1.48382000	0.03626500	54.11542600	0.00098744	0.00098744	0.00077979
28	[31]	Guo et al., 2016	CSO	0.76078000	0.32300000	1.48118000	0.03638000	53.71850000	0.00098602	0.00098612	0.00077544
29	[32]	Hamid et al., 2016	NM-MPSO	0.76078000	0.32306000	1.48120000	0.03638000	53.72220000	0.00098602	0.00098620	0.00077550

#	Ref.	Authors, year	Method	$I_{pv}$ (A)	$I_o$ ( $\mu$ A)	$n$	$R_s$ ( $\Omega$ )	$R_p$ ( $\Omega$ )	Original reported RMSE	RMSE calculated using Eq. (3)	Proposed RMSE calculated using Eq. (12)
30	[33]	Zhang et al., 2016	PCE	0.76077600	0.32302100	1.48107400	0.03637700	53.71852500	0.00098602	0.00106059	0.00080924
31	[34]	Tong et al., 2016	TONG	0.76100000	0.36350000	1.49350000	0.03660000	62.57400000	NG	0.00238593	0.00150509
32	[35]	Jamadi et al., 2016	MABC	0.76077900	0.32132300	1.48138500	0.03638900	53.39999000	0.00098601	0.00276101	0.00172770
33	[36]	Ali et al., 2016	MVO	0.76160000	0.32094000	1.52520000	0.03650000	59.58840000	NG	0.12679796	0.08627778
34	[37]	Chellaswamy et al., 2016	DET	0.75100000	0.31500000	1.48700000	0.03600000	54.53200000	0.00093000	0.02448057	0.01584481
35	[38]	Jordehi, 2016	WCA	0.76090800	0.41355400	1.50438100	0.03536300	57.66948800	0.00094655	0.00760691	0.00464720
36			TLBO	0.76080900	0.31224400	1.47578000	0.03655100	52.84050000	0.00077487	0.00727229	0.00433487
37			GWO	0.76099600	0.24303880	1.45121900	0.03773200	45.11630900	0.00095145	0.00728451	0.00434963
38			TVA-CPSO	0.76078800	0.31068270	1.47525800	0.03654700	52.88964400	0.00077301	0.00734381	0.00436800
39	[39]	Ma et al., 2016	PPSO	0.76080000	0.32300000	1.48120000	0.03640000	53.71850000	NG	0.00099161	0.00077779
40	[40]	Chen et al., 2016	EHA-NMS	0.76080000	0.32302100	1.48118400	0.03637700	53.71852100	0.00098602	0.00098635	0.00077570
41	[41]	Yuan et al., 2015	CARO	0.76079000	0.31724000	1.48168000	0.03644000	53.08930000	0.00098665	0.00819692	0.00495024
42	[42]	Lim et al., 2015	LI	0.76094380	0.34565720	1.48799169	0.03614233	49.48220500	0.00105480	0.00134617	0.00105482
43	[43]	El-Fergany, 2015	MBA	0.76040000	0.23480000	1.48900000	0.03880000	44.61000000	NG	0.11672175	0.07620443
44	[44]	Alam et al., 2015	FPA	0.76079000	0.31067700	1.47707000	0.03654660	52.87710000	0.00077301	0.00121214	0.00087797
45	[45]	Dkhichi et al., 2014	LMSA	0.76078000	0.31849000	1.47976000	0.03643000	53.32644000	0.00098640	0.00098649	0.00077406
46	[46]	Niu et al., 2014	DE	0.76068000	0.35515000	1.49080000	0.03598000	56.55330000	0.00100000	0.00100348	0.00080173
47			BBO	0.76098000	0.86100000	1.58742000	0.03214000	78.85550000	0.00238000	0.00239295	0.00200212
48			BBO-M	0.76078000	0.31874000	1.47984000	0.03642000	53.36227000	0.00098634	0.00098656	0.00077423
49	[47]	Niu et al., 2014	STLBO	0.76078000	0.32302000	1.48114000	0.03638000	53.71870000	0.00098602	0.00099764	0.00078059
50			TLBO	0.76074000	0.32378000	1.48136000	0.03641000	54.40290000	0.00098845	0.00100164	0.00078421
51	[48]	Oliva et al., 2014	ABC	0.76080000	0.32510000	1.48170000	0.03640000	53.64330000	0.00098602	0.00109667	0.00083343
52	[49]	Laudani et al., 2014	HPEPD	0.76078840	0.31024820	1.47696410	0.03655304	52.85905600	0.00077301	0.00114867	0.00084728
53	[50]	Yuan et al., 2014	MPCOA	0.76073000	0.32655000	1.48168000	0.03635000	54.63280000	0.00094457	0.00231307	0.00146916
54	[51]	Patel et al., 2014	TLBO	0.76080000	0.32230000	1.48370000	0.03640000	53.76027000	NG	0.00969602	0.00585540
55	[52]	Askarzadeh et al., 2013	BMO	0.76077000	0.32479000	1.48173000	0.03636000	53.87160000	0.00098608	0.00098622	0.00077621
56	[53]	Askarzadeh et al., 2013	ABSO	0.76080000	0.30623000	1.47583000	0.03659000	52.29030000	0.00099124	0.00099125	0.00077368
57	[54]	Jiang et al., 2013	IADE	0.76070000	0.33613000	1.48520000	0.03621000	54.76430000	0.00098900	0.00099076	0.00078442
58	[55]	Hachana et al., 2013	ABSO	0.76080000	0.30623000	1.47986000	0.03659000	52.29030000	0.00098602	0.01416898	0.00855244
59			ABCDE	0.76077000	0.32302000	1.47986000	0.03637000	53.71850000	0.00098602	0.00485483	0.00292463
60			DE	0.76077000	0.32302000	1.48059000	0.03637000	53.71850000	0.00098602	0.00234235	0.00148100
61			MPSO	0.76077000	0.32302000	1.47086000	0.03637000	53.71850000	0.00098602	0.03902188	0.02247017

#	Ref.	Authors, year	Method	$I_{pv}$ (A)	$I_0$ ( $\mu$ A)	$n$	$R_s$ ( $\Omega$ )	$R_p$ ( $\Omega$ )	Original reported RMSE	RMSE calculated using Eq. (3)	Proposed RMSE calculated using Eq. (12)
62	[56]	Askarzadeh et al., 2012	GGHS	0.76092000	0.32620000	1.48217000	0.03631000	53.06470000	0.00099097	0.00099089	0.00078146
63			HS	0.76070000	0.30495000	1.47538000	0.03663000	53.59460000	0.00099510	0.00099515	0.00077625
64			IGHS	0.76077000	0.34351000	1.48740000	0.03613000	53.28450000	0.00099306	0.00103345	0.00082116
65	[57]	Gong et al., 2013	Rcr-IJADE	0.76077600	0.32302100	1.48118400	0.03637700	53.71852600	0.00098602	0.00098602	0.00077539
66	[58]	AlHajri et al., 2012	PS	0.76170000	0.99800000	1.60000000	0.03130000	64.10256000	0.28630000	0.01493638	0.00981702
67	[59]	El-Naggar et al., 2012	SA	0.76200000	0.47980000	1.51720000	0.03450000	43.10345000	0.00170000	0.01899784	0.01165472
68	[60]	AlRashidi et al., 2011	GA	0.76190000	0.80870000	1.57510000	0.02990000	42.37288000	NG	0.01907803	0.01200884
69	[61]	Ye et al., 2009	PSO	0.76079800	0.32272100	1.48382000	0.03639400	53.79650000	NG	0.00965452	0.00583097

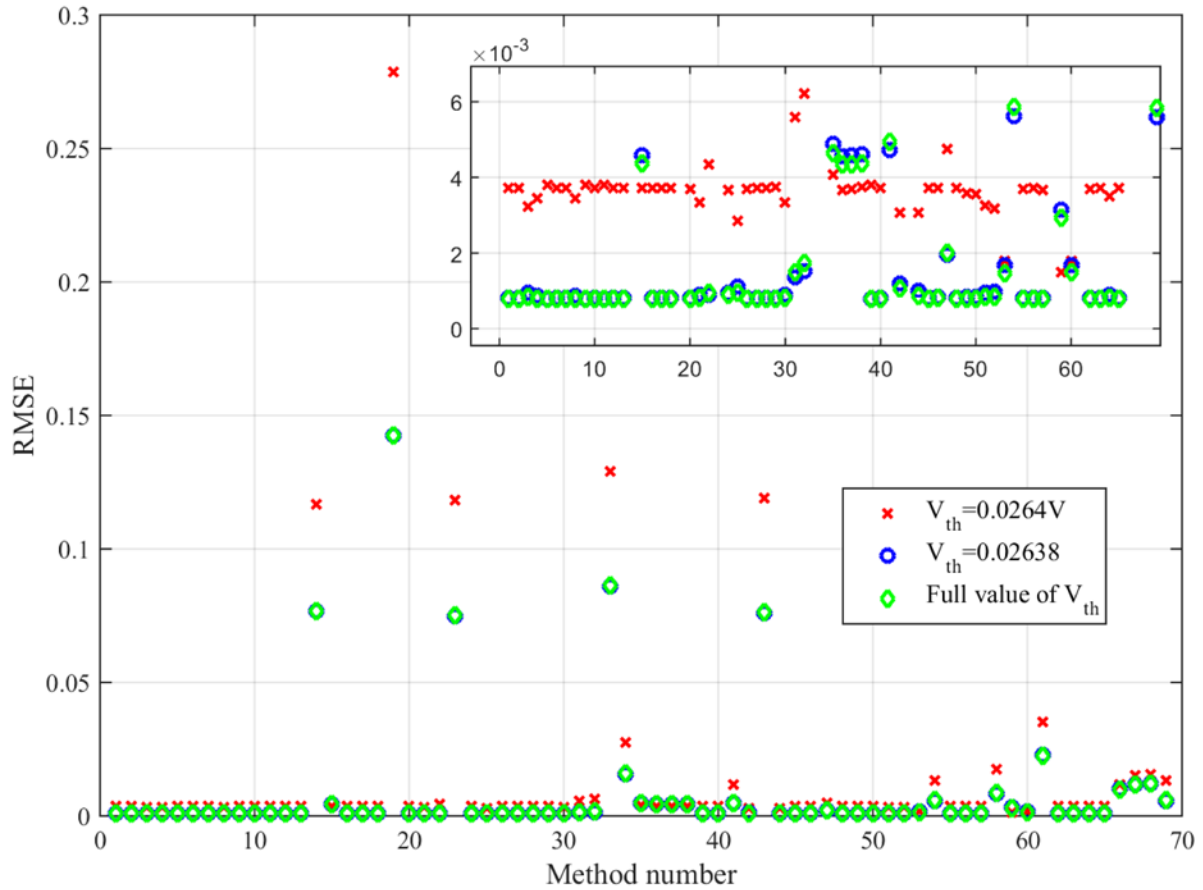
346 \*NG: not given





347  
 348  
 349

Fig. 3. The difference in a logarithmic scale between proposed RMSE values calculated using Eq. (12) and those calculated using different methods presented in the literature (Method number after Table 1)



350  
 351 Fig. 4. Impact of  $V_{th}$  value on the RMSE value calculated using Eq. (12) (Method  
 352 number after Table 1)  
 353

354 Based on the results shown in Table 1, we can see that the most accurate method for  
 355 parameter estimation of single diode RTC France solar cell is the HISA method (method  
 356 number 2) presented by *Kler* et al. in 2019 [5]. The results of this method are given in bold in  
 357 Table 1. The  $I-U$  characteristic of the RTC France solar cells obtained for these parameters, as  
 358 well as the measured characteristic, are shown in Fig. 5, in which the remarkable agreement  
 359 between the measured and simulated characteristics is indicated.

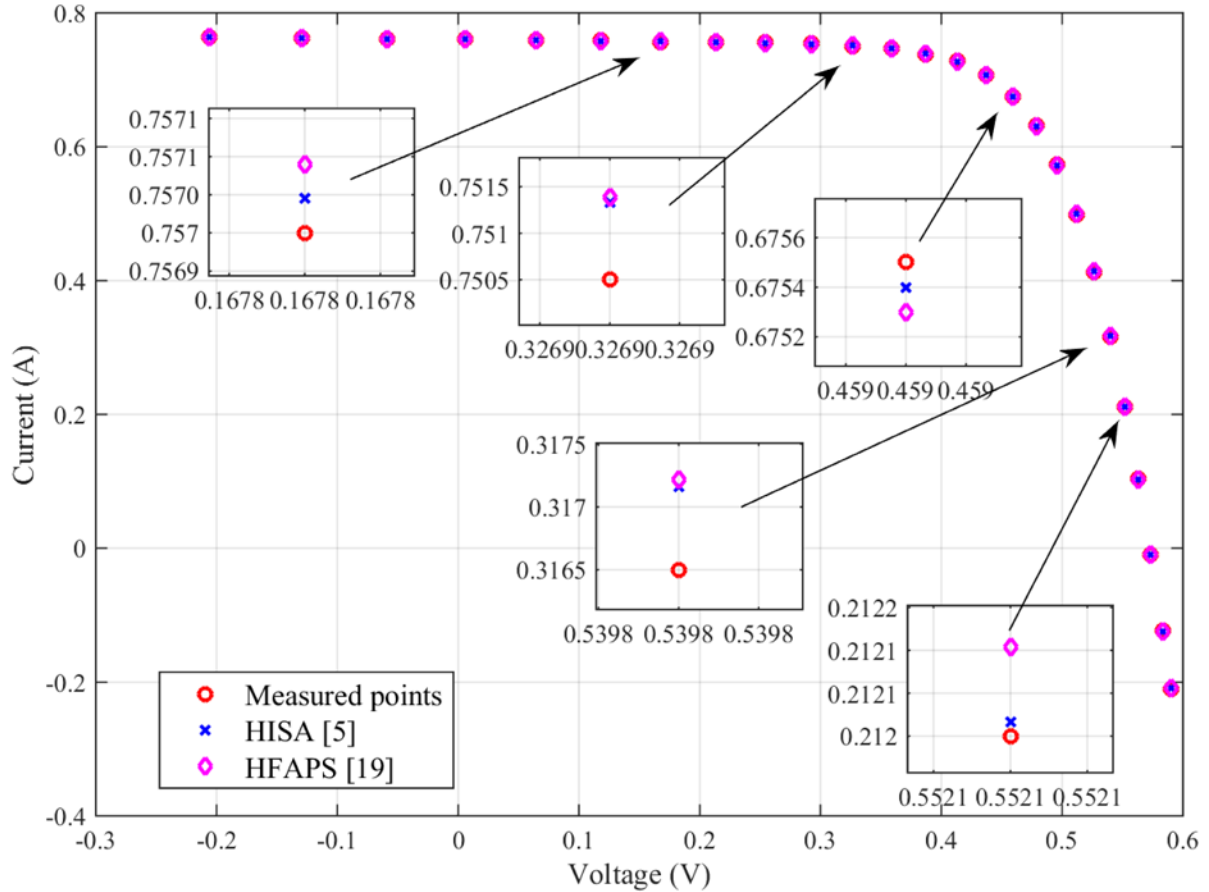
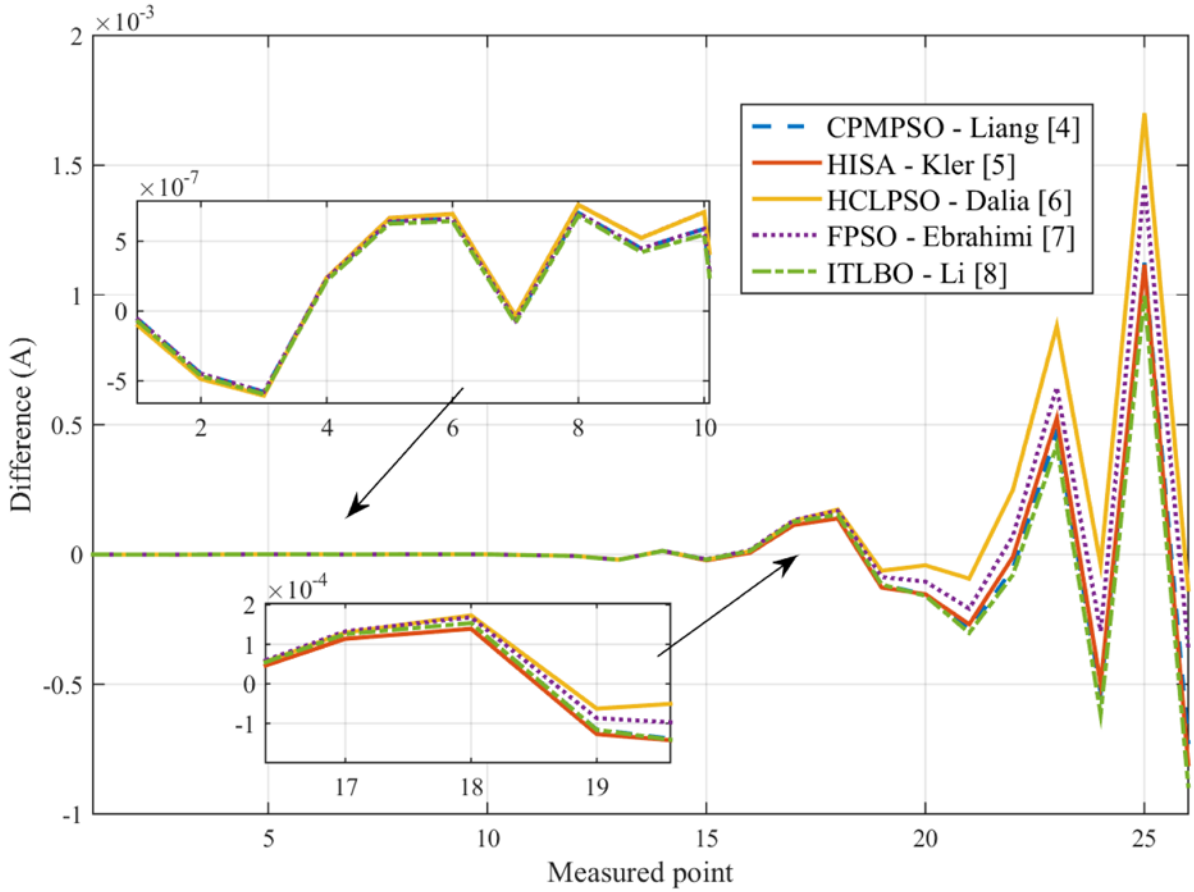


Fig. 5. Current-voltage characteristic of the RTC France solar cell

360  
361

362 In order to show that the proposed method provides the best response, the characteristics  
 363 of parameters determined using the HFAPS method (number 16) presented in [19], which also  
 364 has good accuracy, is shown in the same figure. It is evident from the figure that a lower value  
 365 of RMSE guarantees better matching between measured and estimated characteristics. The  
 366 Matlab code for calculating  $I-U$  characteristics of the RTC solar cell parameters determined  
 367 using the HFAPS method, method number 16 in [19], is presented in Appendix 2.

368 Furthermore, the relative difference between the current calculated using the proposed  
 369 formula expressed in Eq. (9) and the conventional, erroneous, one expressed in Eq. (3), for the  
 370 solar cell parameters presented, is shown in Fig. 6. Yet again, it is clear that there is a  
 371 considerable difference in solar cell current values between the two formulas. Also, it evidences  
 372 the importance of the proposed RMSE expression to develop a good base for proper  
 373 investigation and implementation of optimization algorithms to solve the 5-parameter  
 374 estimation problem of single diode PV equivalent circuits.



375

376

Fig. 6. The difference in current values calculated by Eq. (3) and last part of Eq. (9)

377

*Precision of calculation of the methods used for analytical solving of the Lambert W equation*

378

379

380

381

382

383

384

As mentioned before, for solving a Lambert  $W$  function, two methods, TS and STFT, are used. An investigation of the impact of  $\beta$  on the accuracy of the solution is presented. Fig. 7 shows a 3D illustration of  $\beta$ , measured points from the  $I-U$  characteristics of the RTC solar cell, and methods presented in Table 1. From the same figure, one can note that the minimal value of  $\beta$  is  $1.46 \times 10^{-9}$ , while the maximal value of  $\beta$  is 3.52. For that reason, some solutions to the Lambert  $W$  equation are obtained using TS and others are obtained using STFT. In this section, all calculations are performed in the environment of *Mathematica*.

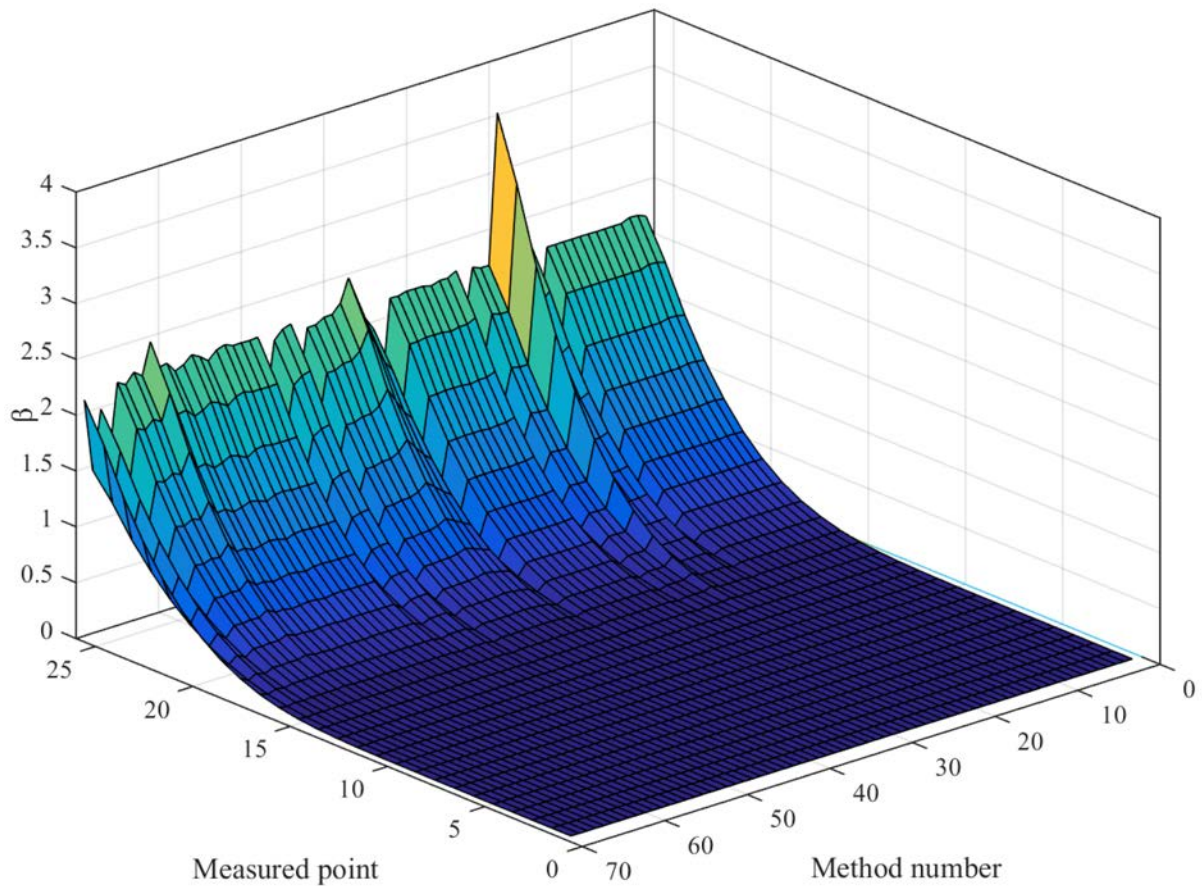
385

386

The precision of calculation  $Pr$  that reflects accuracy, either based on TS or STFT ( $Pr_{STFT}$  and  $Pr_{Taylor}$ ), is given as follows [72]:

$$Pr = \left| 1 - \log \left( \left| x - \beta \exp(-x) \right| \right) \right| \quad (12)$$

387 Namely, for the high values of  $Pr$ , the accuracy of the solution is high. Table 2 presents  
 388  $Pr_{STFT}$  and  $Pr_{Taylor}$  for different values of  $\beta$ .



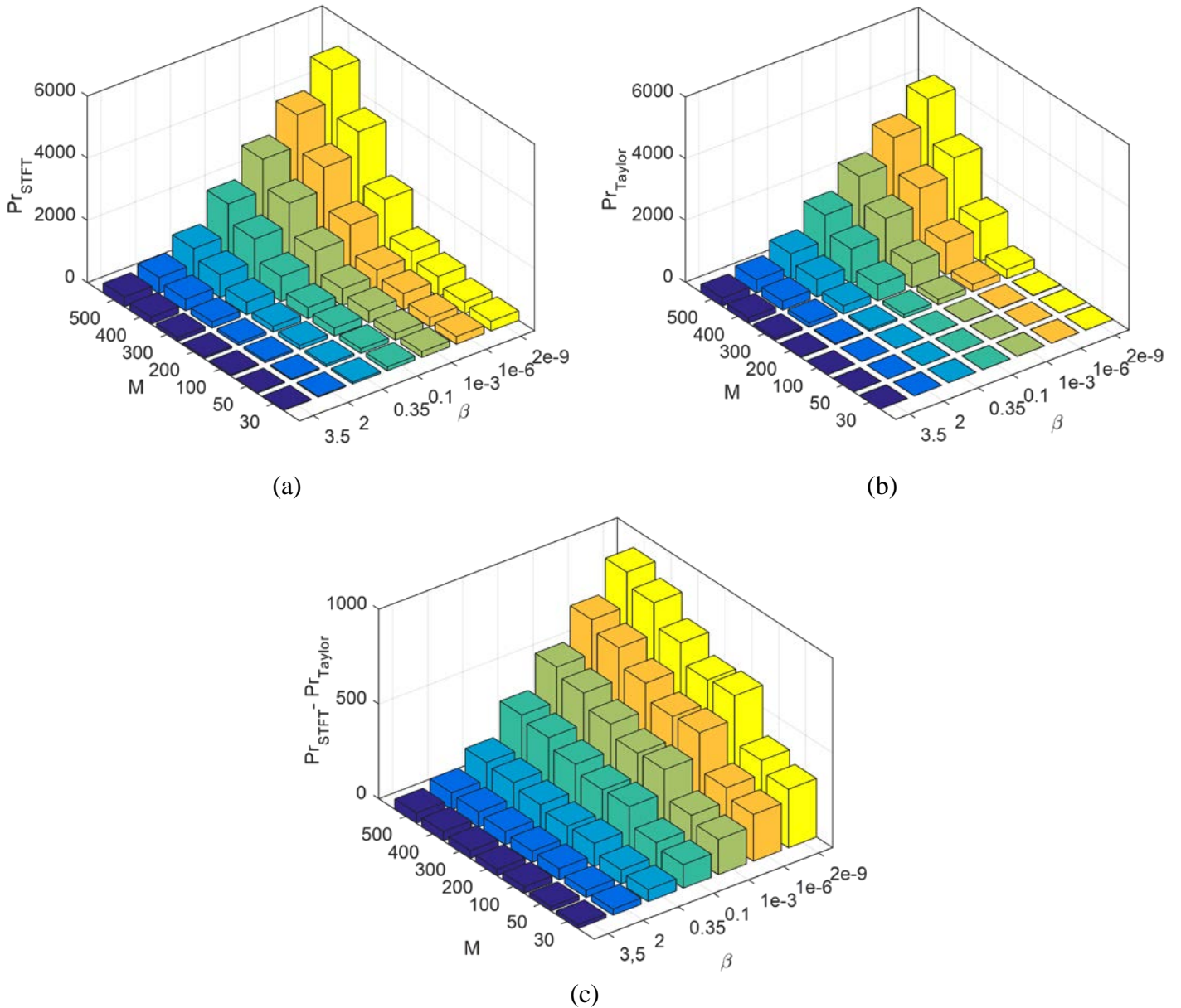
389  
 390 Fig. 7. 3D graph of  $\beta$ , measured points from the  $I-U$  characteristics of the RTC solar cell, and  
 391 methods in Table 1

392 It should be noted that the peak region present in Fig. 7 is due to the parameters obtained  
 393 using method 19 reported in Table 1 as the values of  $I_0$  and  $n$  obtained using method 19 were  
 394 quite different from the corresponding values obtained using the other methods.

395 It can be seen that higher precision can be obtained if we use STFT for solving the  
 396 Lambert  $W$  equation. Furthermore, for a higher value of  $\beta$ , TS cannot be used. Recalling Eqs.  
 397 (7) and (8), it should be noted that for the same value of integer  $M$ , the STFT gives much more  
 398 accurate results than TS. Also, the higher the value of  $M$ , the higher the accuracy is. The  
 399 difference between the accuracy of  $Pr_{STFT}$  and  $Pr_{Taylor}$  for different values of  $\beta$  and  $M$  is  
 400 illustrated in Fig. 8.

Table 2.  $Pr_{STFT}$  and  $Pr_{Taylor}$  for different values of  $M$  and  $\beta$ 

$\beta$	Solution, $x$	$M$	$Pr_{STFT}$	$Pr_{Taylor}$
$2 \times 10^{-9}$	1.9999999960000000, $1199994253 \times 10^{-9}$	30	314	260
		50	515	426
		100	1019	840
		200	2025	1667
		300	3033	2493
		400	4039	3320
$1 \times 10^{-6}$	9.9999900000149999, $7333338541 \times 10^{-7}$	30	225	177
		50	370	288
		100	732	567
		200	1455	1124
		300	2177	1681
		400	2901	2237
		500	3624	2794
$1 \times 10^{-3}$	0.0009990014973385, 3088995782715	30	125	84
		50	205	135
		100	405	264
		200	804	521
		300	1203	778
		400	1604	1034
		500	2002	1291
0.1	0.0912765271608622, 6429989572142	30	57	22
		50	93	33
		100	182	62
		200	361	119
		300	540	176
		400	719	233
		500	897	289
0.35	0.2677773400403608, 4269261612680	30	40	5
		50	66	6
		100	129	7
		200	255	10
		300	381	12
		400	508	15
		500	634	17
2	0.8526055020137254, 9134647241469	30	23	0
		50	38	0
		100	75	0
		200	148	0
		300	221	0
		400	295	0
		500	368	0
3.5	1.1302893269741358, 2651855880912	30	20	0
		50	32	0
		100	63	0
		200	124	0
		300	186	0
		400	247	0
		500	309	0



402 Fig. 8.  $Pr_{STFT}$  and  $Pr_{Taylor}$  for different values of  $\beta$  and  $M$ : (a)  $Pr_{STFT}$ , (b)  $Pr_{Taylor}$ , and (c)

403  $Pr_{STFT} - Pr_{Taylor}$

404 **4. Application of the solution methodology**

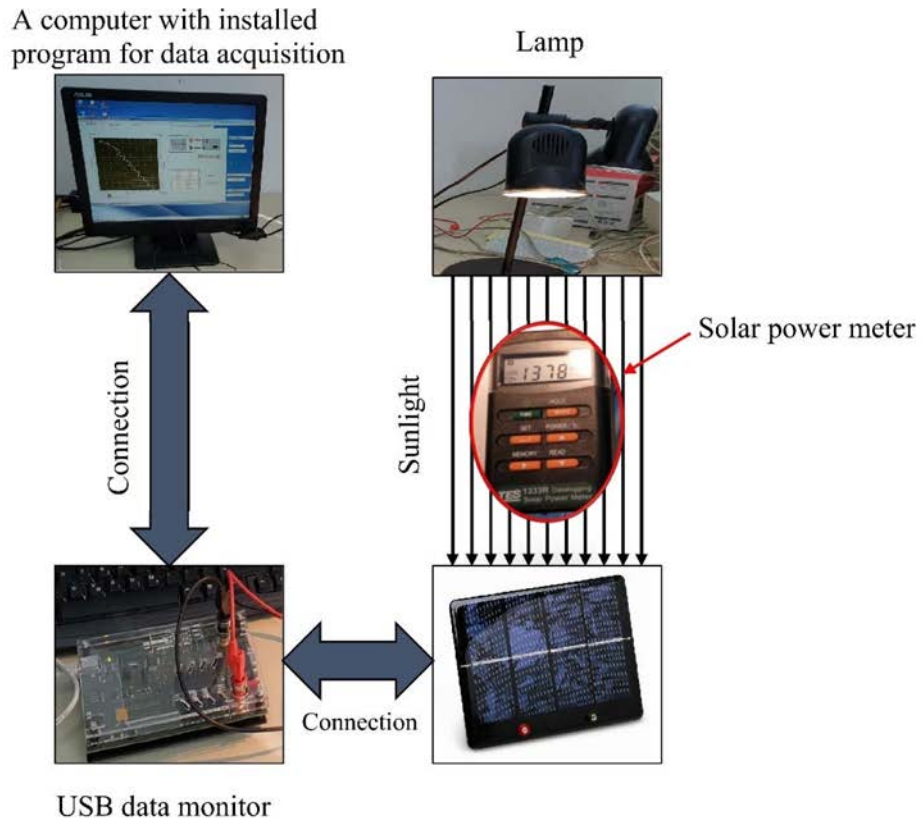
405 *Experimental setup and parameters estimation of solar modules of clean energy trainer setup*

406 In order to validate the solution methodology, the experimental results of a Clean Energy  
 407 Trainer Setup module in the Laboratory of automatics at the University of Montenegro are  
 408 presented and discussed, and the single diode parameters of the considered module are  
 409 estimated. The experimental setup, shown in Fig. 9, consists of a computer with installed  
 410 software for data acquisition and analysis, TES 1333R data logging solar power meter with  
 411 high irradiance ( $G$ ) resolution ( $0.1 \text{ W/m}^2$ ), lamp for sunlight simulation, USB data monitor for  
 412 data acquisition purposes, and two modules of solar cells.

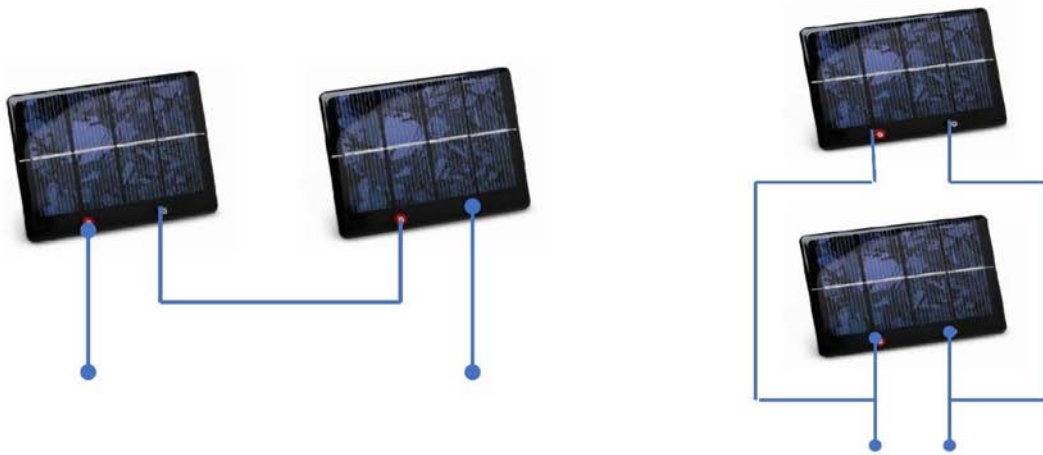
413           The  $I-U$  characteristic of one solar module at  $G$  equals  $1330 \text{ W/m}^2$  and a temperature  
414 of  $39 \text{ }^\circ\text{C}$  is measured. The 5 parameters to be determined are not directly addressed by the  
415 current methodology; however, the optimization techniques rely on objective functions whose  
416 accuracy can be improved by the proposed RMSE calculation. Then, for the measured  $I-U$   
417 pairs, the 5-parameter single diode solar cell parameters are estimated using three optimization  
418 approaches, namely COA [13], ER-WCA [23], and HS [55,74]. The reader can refer to  
419 [13,23,55] for more details about these algorithms. The results obtained are presented in Table  
420 3, in which all the values obtained using Eq. (12) are within their fitness function.

421           It can be seen from Table 3 that the results obtained using the optimization techniques  
422 are close to each other, in which all the values obtained using Eq. (12) are within their fitness  
423 function. However, the COA method gives the best accuracy in terms of RMSE. The simulated  
424 and measured  $I-U$  characteristics via the parameters obtained using the different optimization  
425 methods at  $G=1330 \text{ W/m}^2$  and  $T=39 \text{ }^\circ\text{C}$  are shown in Fig. 10.





(a)



(b)

(c)

426

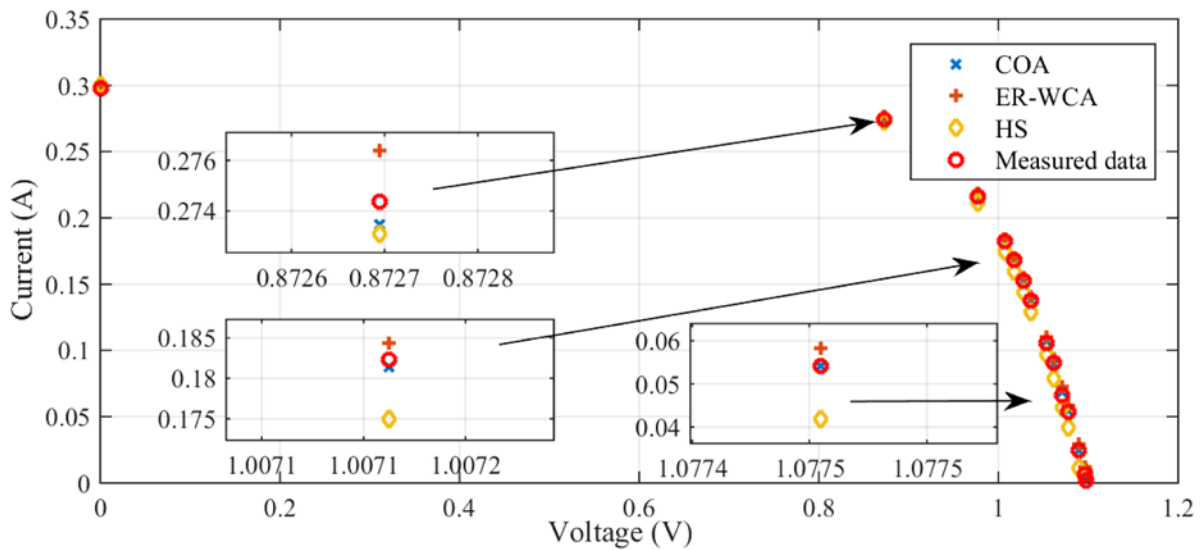
427

428

Fig. 9. Experimental setup: (a) Connection, (b) Series connection of solar modules, and (c) Parallel connection of solar modules

429 Table 3. Experimental results obtained from the tested solar module (Number of runs to  
 430 achieve the optimum parameters for ER-WCA is 50, and 100 for COA and HS)

Parameters/Algorithm	COA	ER-WCA	HS
$R_S$ ( $\Omega$ )	0.114	0.121	0.114
$R_P$ ( $\Omega$ )	219.75	236.10	222.54
$I_o$ (A)	$10.56 \times 10^{-8}$	$9.13 \times 10^{-8}$	$12.13 \times 10^{-8}$
$I_{pv}$ (A)	0.2987	0.3012	0.3001
$n$	0.3441	0.3411	0.3456
RMSE calculated using Eq. (3)	0.00152416	0.00543925	0.01303987
Proposed RMSE calculated using Eq. (12)	0.00113727	0.00397174	0.00955046

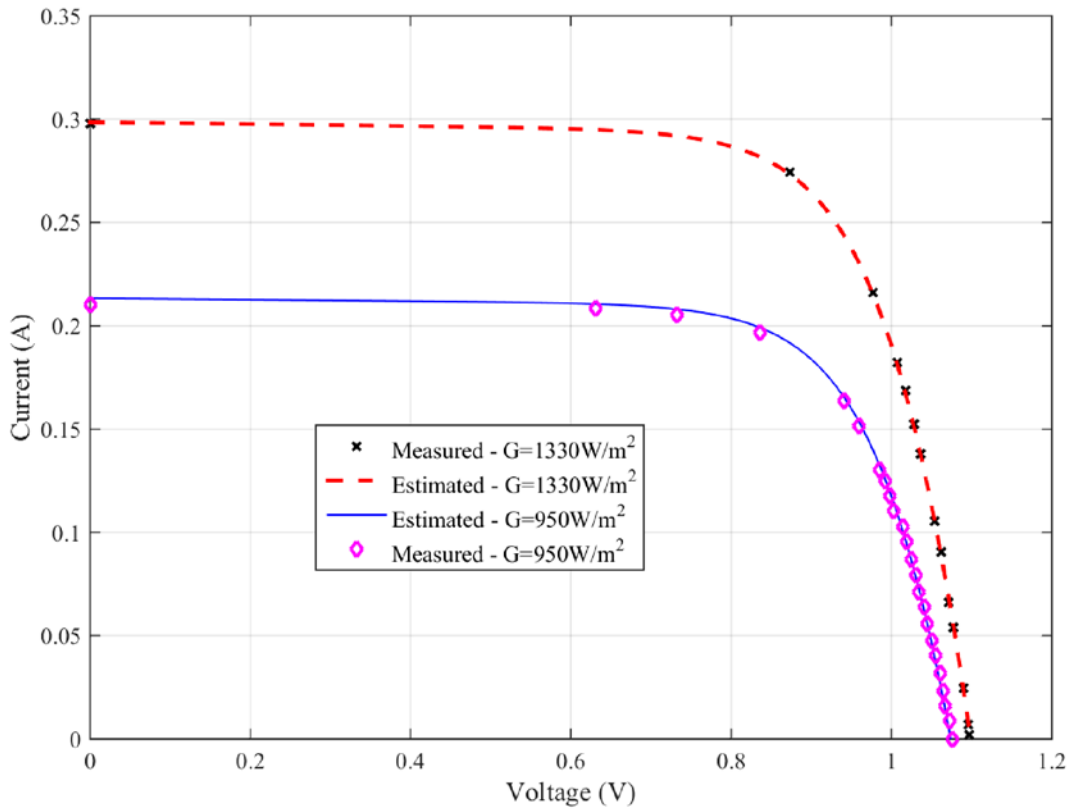


431  
 432 Fig. 10. The  $I-U$  characteristics of one solar module for parameters obtained using the three  
 433 methods ( $G=1330 \text{ W/m}^2$  and  $T=39 \text{ }^\circ\text{C}$ )

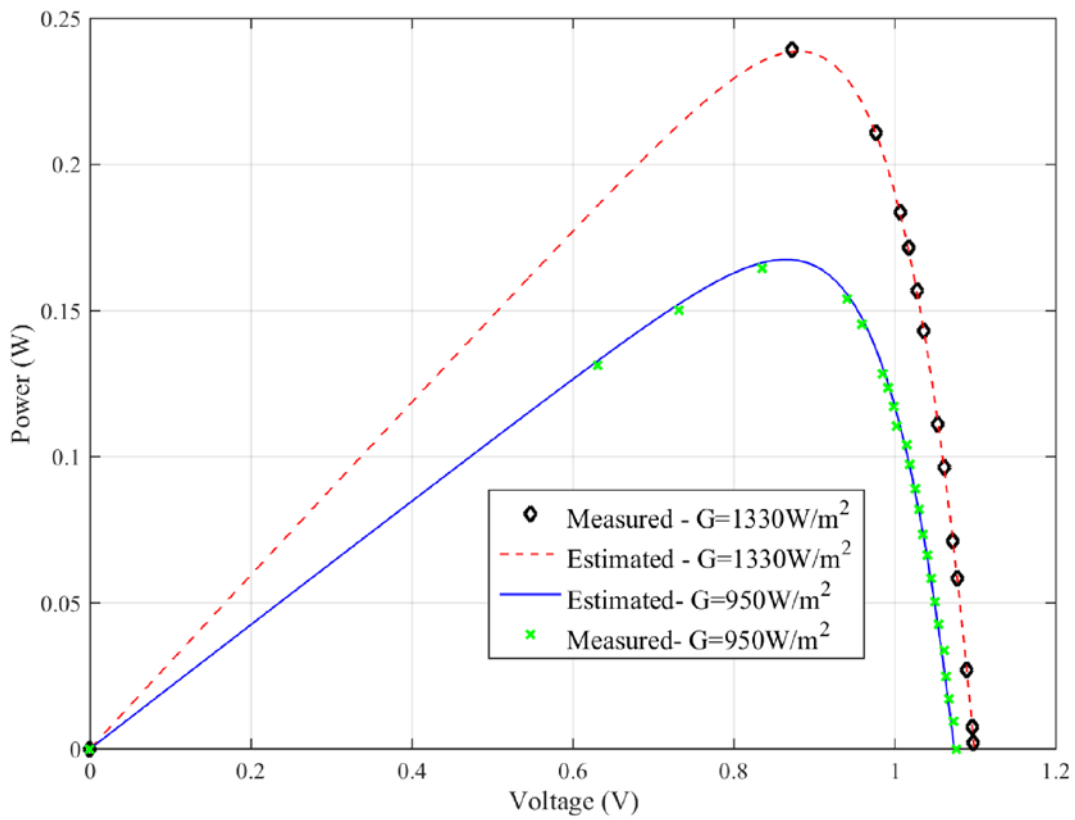
434 Besides, the  $I-U$  and  $P-U$  characteristics of one module at two different irradiance values  
 435 at the same temperature ( $T = 39 \text{ }^\circ\text{C}$ ), are presented in Fig. 11, respectively. In addition, the  $I-U$   
 436 and  $P-U$  characteristics for series and parallel connection of the modules are presented in  
 437 Fig. 12. The agreement between both measured and estimated characteristics is remarkable for  
 438 all presented figures. It should be noted that all the characteristics are presented for data  
 439 obtained using the COA method while taking into consideration the change of parameters with  
 440 irradiance and temperature [75].

441 *Proposed RMSE expression and parameters estimation of Solarex MSX-60 PV solar module*

442 In Table 4, for Solarex MSX-60 PV solar module, RMSE values calculated using the erroneous  
 443 Eq. (3) as well as the RMSE values calculated using Eq. (12), are presented. Also, in the same  
 444 table, the estimated values of the solar cell parameters using COA, ER-WCA, and HS, as well  
 445 as estimated values of different methods in the literature are presented.



(a)



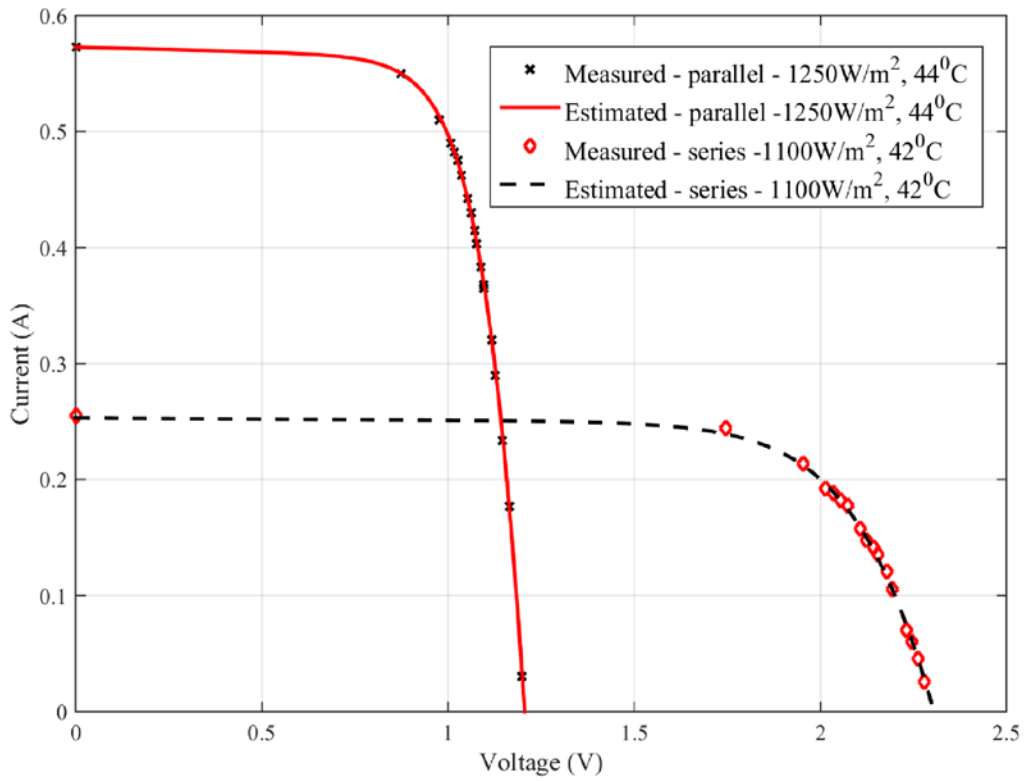
(b)

446  
447

448  
449

450  
451

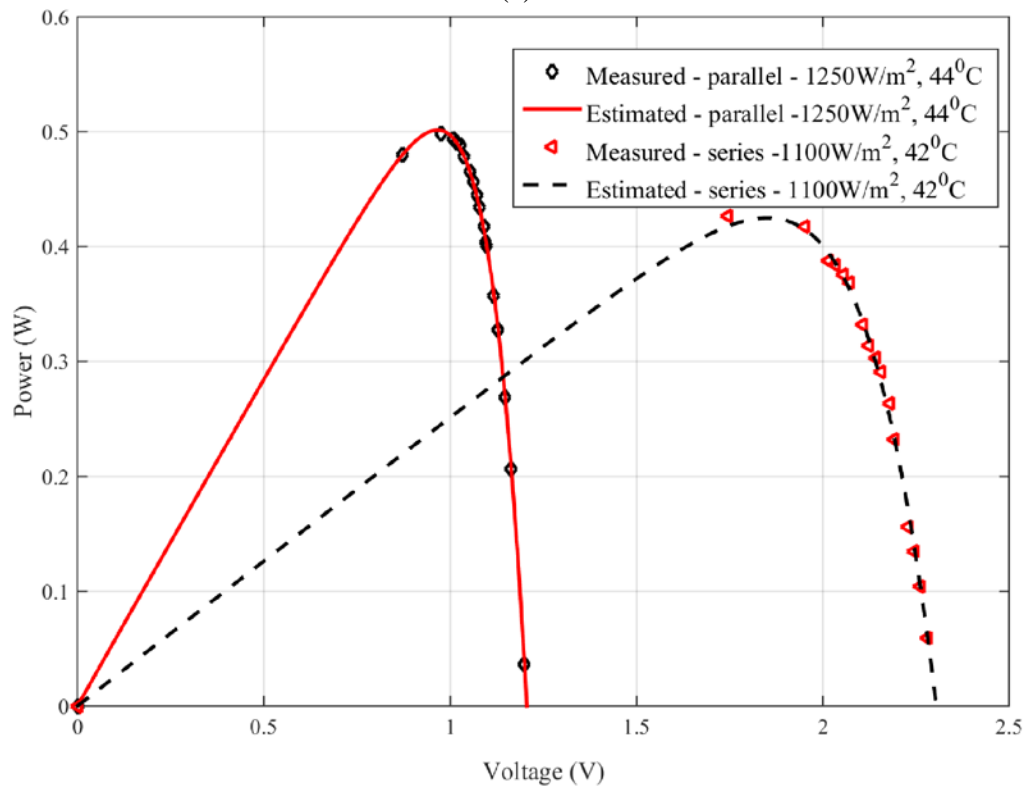
Fig. 11. The characteristics of one module at two different irradiance values at the same temperature ( $T = 39\text{ }^{\circ}\text{C}$ ): (a)  $I-U$  characteristic and (b)  $P-U$  characteristic



452

453

(a)



454

455

(b)

456

Fig. 12. The characteristics of series and parallel connections of modules: (a)  $I-U$

457

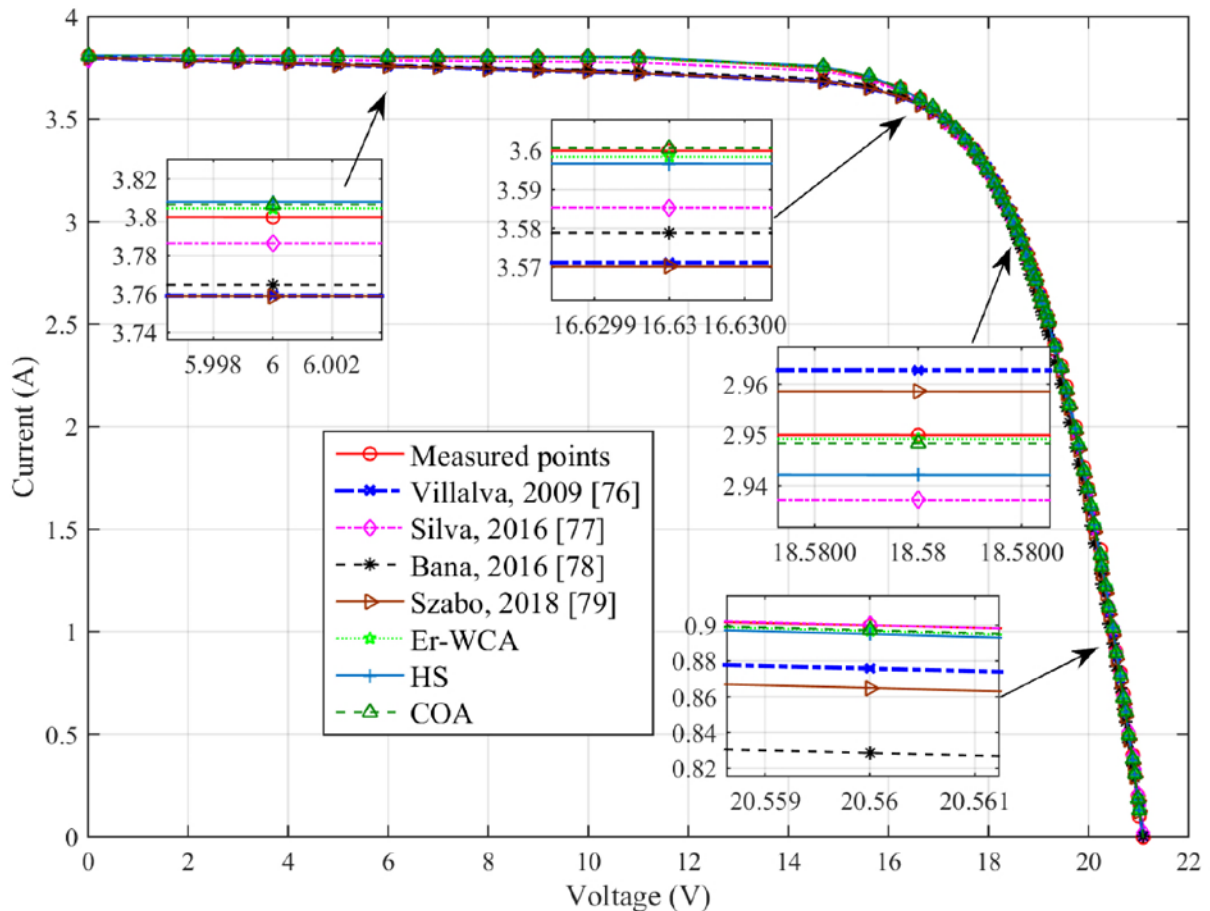
characteristic and (b)  $P-U$  characteristic

458  
459

Table 4. Numerical results of the conventional and proposed RMSE for parameters estimation of Solarex MSX–60 PV solar module (Results with the minimum RMSE using the proposed approach are given in bold)

#	Ref.	Authors, year	Method	$I_{pv}$ (A)	$I_0$ (A)	$n$	$R_S$ ( $\Omega$ )	$R_P$ ( $\Omega$ )	RMSE calculated using Eq. (3)	Proposed RMSE calculated using Eq. (12)
1	[76]	Villalva et al., 2009	A&I	3.8082	0.0000000012	1.0453	0.3160	146.081	0.03611840076252	0.02839662736179
2	[77]	Silva et al., 2016	A&I	3.7983	0.0000000679	1.2800	0.2510	582.728	0.02502525341693	0.01810661464843
3	[78]	Bana et al., 2018	NM	3.8084	0.0000000005	1.0003	0.3692	169.047	0.09613294311904	0.05563692889594
4	[79]	Szabo et al., 2018	BC	3.8080	0.0000000012	1.0450	0.3160	146.080	0.04202673823244	0.03072250565403
5	<b>Proposed</b>	<b>ER-WCA</b>	<b>3.8121</b>	<b>0.0000001399</b>	<b>1.3325</b>	<b>0.2235</b>	<b>914.689</b>	<b>0.01697330882512</b>	<b>0.01697330882512</b>	
6		HS	3.8115	0.0000002265	1.3707	0.2129	1976.070	0.01775687114902	0.01775687114902	
7		COA	3.8100	0.0000001783	1.3514	0.2184	2004.977	0.01705021261682	0.01705021261682	

460 It can be seen from Table 4 that the differences between the proposed and conventional  
 461 RMSE values are considerable. The  $I-U$  characteristics of the Solarex MSX-60 module are  
 462 shown in Fig. 13, in which the agreement between both measured and estimated characteristics  
 463 is remarkable for all the presented methods. However, it is noted that the results obtained using  
 464 the ER-WCA method are the closest to the measured values. This is also validated by the  
 465 proposed RMSE value calculated using Eq. (12) in Table 4, as the minimum RMSE value  
 466 (0.011706768459604) is obtained using this method (method 5 given in bold in Table 4).



467  
 468 Fig. 13. The  $I-U$  characteristics of the Solarex MSX-60 module

469 Furthermore, the relative difference of the current in amperes calculated by Eq. (3) and  
 470 last part of Eq. (9), for the parameters of Solarex MSX-60 module presented, is shown in Fig.  
 471 14. Yet again, it is clear that there is a considerable difference in solar cell current values  
 472 between the two formulas, in which the difference in the solar cell current values shows the  
 473 error in the conventional calculation methods since the exact expression of the calculated cell  
 474 output current is not used. Other promising optimization techniques such as hybrid and  
 475 improved algorithms [80-83] can be employed to address the problem using the proposed  
 476 RMSE expression to get better solutions.

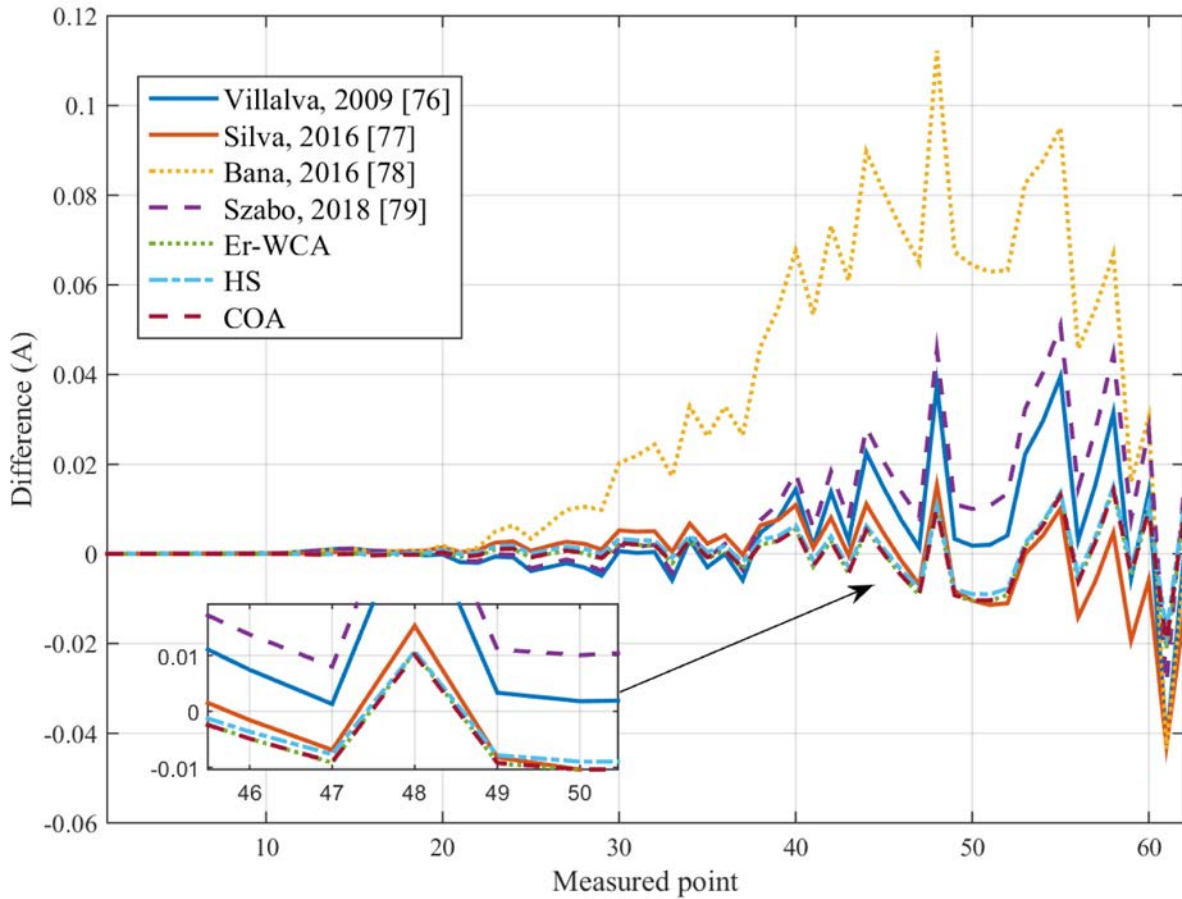


Fig. 14. The difference in current values calculated by Eq. (3) and last part of Eq. (9)

## 5. Conclusions

In the available literature, one can find a lot of methods and techniques employed to estimate single diode solar PV cell parameters. In this work, values of RMSE of RTC France solar PV cell and Solarex MSX-60 module are presented and discussed. We proposed an exact analytical solution for RMSE calculation based on the Lambert  $W$  function. The results obtained show that the RMSE values were not calculated correctly in most of the methods presented in the literature since the exact expression of the calculated cell output current was not used. The precision of two numerical approaches to numerically solve the Lambert  $W$  function is also addressed with: (i) one based on TS; and (ii) the other based on STFT. In addition, the impact of the thermal voltage on RMSE calculation is addressed. Further, the applicability of the proposed solution methodology is explored with the aid of the experimental results. It was found that the reasons for results mismatching of the minimum RMSE in the published papers are not using all the measured points for RMSE calculation, complete dependence on optimization techniques to reach a solution, approximation of the values of the operational factors and inaccurate solving of the Lambert  $W$  function. In regard to double and triple diode

495 PV equivalent circuits, no exact analytical solution has been reached yet because of the high  
 496 nonlinearity of the current expressions of these models. Finally, this work aimed to develop a  
 497 good base for proper investigation and implementation of optimization algorithms to solve the  
 498 parameter estimation problem of 5-parameter single diode PV equivalent circuits.

## 499 APPENDIX 1

### 500 A1.1 Matlab code for solving Lambert W equation

501 The central part of the Matlab code for RMSE calculation based on the Lambert W function is  
 502 given in Appendix 1 as follows [17,27]:

```

503 % RTC FRANCE CURRENTS
504 Iiz=[0.7640 0.7620 0.7605 0.7605 0.7600 0.7590 0.7570 0.7570 0.7555 0.7540 0.7505 0.7465
505 0.7385 0.7280 0.7065 0.6755 0.6320 0.5730 0.4990 0.4130 0.3165 0.2120 0.1035 -0.0100 -
506 0.1230 -0.2100];
507 % RTC FRANCE VOLTAGES
508 Uiz=[-0.2057 -0.1291 -0.0588 0.0057 0.0646 0.1185 0.1678 0.2132 0.2545 0.2924 0.3269
509 0.3585 0.3873 0.4137 0.4373 0.4590 0.4784 0.4960 0.5119 0.5265 0.5398 0.5521 0.5633
510 0.5736 0.5833 0.5900];
511 % Number of measured points
512 N=length(Uiz);
513 % define Rp, Rs, Vth, a – Ideality factor, Io, Ipv, ...
514 for t=1:N
515     BETA=Io*10^-6*Rs*Rp/(a*Vth*(Rs+Rp))*exp((Rp*(Rs*Ipv+Rs*Io*10^-
516 6+Uiz(t)))/(a*Vth*(Rs+Rp)));
517     CHECKING(t)=lambertw(BETA)- BETA *exp(-lambertw(BETA));
518     CURRENTCALCULATED=(Rp*(Ipv+Io*10^-6)-Uiz(t))/(Rs+Rp)-
519 a*Vth*lambertw(BETA)/Rs;
520     ERROR(t)=(CURRENTCALCULATED-Iiz(t))^2;
521 End
522 RMSE=sqrt(sum(ERROR)/N)
  
```



## 523 **A1.2 Mathematica code for solving Lambert W equation**

```
524 digitnumber=1000;
525 beta=35/10;
526
527 M=30;
528 Print["M= ", M];
529 F1= $\sum_{x=0}^M (\text{beta}^x * (((M-x)^x) / x!));$ 
530 F2= $\sum_{x=0}^{M+1} (\text{beta}^x * (((M+1-x)^x) / x!));$ 
531 SolutionTRANS = SetPrecision[beta*(F1/F2), digitnumber];
532 Print["SolutionTRANS= ", SolutionTRANS]
533 ErrorTRANS=SetPrecision[Abs[SolutionTRANS-beta*E^(-SolutionTRANS)], digitnumber];
534 Print["ErrorTRANS= ", ErrorTRANS]
535 solutionLAMBERT =  $\sum_{x=1}^M (\text{beta}^x * (((-x)^{(x-1)}) / x!));$ 
536 Print["solutionLAMBERT= ", SetPrecision[solutionLAMBERT, digitnumber]];
537 ErrorLAMBERT=SetPrecision[Abs[solutionLAMBERT-beta*E^(-solutionLAMBERT)],
538 digitnumber];
539 Print["ErrorLAMBERT= ", ErrorLAMBERT]
540 lambertMATH=N[ProductLog[beta],M]
541 Print["SOLUTIONlambertMATH= ",SetPrecision[lambertMATH, digitnumber]]
542 ErrorPRODUCT=Abs[lambertMATH-beta*E^(-lambertMATH)];
543 Print["ErrorPRODUCT= ",SetPrecision[ErrorPRODUCT, digitnumber]]
```

## 544 **APPENDIX 2**

### 545 **A2. Matlab code for calculating $I-U$ characteristics of the RTC solar cell**

```
546 Ipv=0.76077700
547 Io=0.32262200
548 a=1.48106000
549 Rs=0.03638190
550 Rp=53.67840000
551 for t=1:N
552     BETA=Io*10^-6*Rs*Rp/(a*Vth*(Rs+Rp))*exp((Rp*(Rs*Ipv+Rs*Io*10^-
553 6+Uiz(t)))/(a*Vth*(Rs+Rp)));
554     CHECKING(t)=lambertw(BETA)- BETA *exp(-lambertw(BETA));
555     Icalc(t)=(Rp*(Ipv+Io*10^-6)-Uiz(t))/(Rs+Rp)-a*Vth*lambertw(BETA)/Rs;
556 end
```

### 557 **Funding sources**

558 This research did not receive any specific grant from funding agencies in the public,  
559 commercial, or not-for-profit sectors.

560 **References**

- 561 [1] A.G.E. Mousa, S.H.E. Abdel Aleem, A.M. Ibrahim, Mathematical Analysis of  
562 Maximum Power Points and Currents Based Maximum Power Point Tracking in Solar  
563 Photovoltaic System: A Solar Powered Water Pump Application, *Int. Rev. Electr. Eng.*  
564 11 (2016) 97. doi:10.15866/iree.v11i1.8137.
- 565 [2] S.M. Ismael, S.H.E. Abdel Aleem, A.Y. Abdelaziz, A.F. Zobaa, State-of-the-art of  
566 hosting capacity in modern power systems with distributed generation, *Renew. Energy.*  
567 130 (2019) 1002–1020. doi:10.1016/j.renene.2018.07.008.
- 568 [3] H.G.G. Nunes, J.A.N. Pombo, P.M.R. Bento, S.J.P.S. Mariano, M.R.A. Calado,  
569 Collaborative swarm intelligence to estimate PV parameters, *Energy Convers. Manag.*  
570 185 (2019) 866–890. doi:10.1016/j.enconman.2019.02.003.
- 571 [4] J. Liang, S. Ge, B. Qu, K. Yu, F. Liu, H. Yang, P. Wei, Z. Li, Classified perturbation  
572 mutation based particle swarm optimization algorithm for parameters extraction of  
573 photovoltaic models, *Energy Convers. Manag.* 203 (2020) 112138.  
574 doi:10.1016/j.enconman.2019.112138.
- 575 [5] D. Kler, Y. Goswami, K.P.S. Rana, V. Kumar, A novel approach to parameter  
576 estimation of photovoltaic systems using hybridized optimizer, *Energy Convers.*  
577 *Manag.* 187 (2019) 486–511. doi:10.1016/j.enconman.2019.01.102.
- 578 [6] D. Yousri, D. Allam, M.B. Eteiba, P.N. Suganthan, Static and dynamic photovoltaic  
579 models' parameters identification using Chaotic Heterogeneous Comprehensive  
580 Learning Particle Swarm Optimizer variants, *Energy Convers. Manag.* 182 (2019) 546–  
581 563. doi:10.1016/j.enconman.2018.12.022.
- 582 [7] S.M. Ebrahimi, E. Salahshour, M. Malekzadeh, Francisco Gordillo, Parameters  
583 identification of PV solar cells and modules using flexible particle swarm optimization  
584 algorithm, *Energy.* 179 (2019) 358–372. doi:10.1016/j.energy.2019.04.218.
- 585 [8] S. Li, W. Gong, X. Yan, C. Hu, D. Bai, L. Wang, L. Gao, Parameter extraction of  
586 photovoltaic models using an improved teaching-learning-based optimization, *Energy*  
587 *Convers. Manag.* 186 (2019) 293–305. doi:10.1016/j.enconman.2019.02.048.
- 588 [9] X. Chen, H. Yue, K. Yu, Perturbed stochastic fractal search for solar PV parameter  
589 estimation, *Energy.* 189 (2019) 116247. doi:10.1016/j.energy.2019.116247.
- 590 [10] H. Chen, S. Jiao, A.A. Heidari, M. Wang, X. Chen, X. Zhao, An opposition-based sine  
591 cosine approach with local search for parameter estimation of photovoltaic models,  
592 *Energy Convers. Manag.* (2019). doi:10.1016/j.enconman.2019.05.057.

- 593 [11] N. Pourmousa, S.M. Ebrahimi, M. Malekzadeh, M. Alizadeh, Parameter estimation of  
594 photovoltaic cells using improved Lozi map based chaotic optimization Algorithm, *Sol.*  
595 *Energy*. 180 (2019) 180–191. doi:10.1016/j.solener.2019.01.026.
- 596 [12] S. Li, W. Gong, X. Yan, C. Hu, D. Bai, L. Wang, Parameter estimation of photovoltaic  
597 models with memetic adaptive differential evolution, *Sol. Energy*. (2019).  
598 doi:10.1016/j.solener.2019.08.022.
- 599 [13] M. Čalasan, D. Jovanović, V. Rubežić, S. Mujović, S. Đukanović, Estimation of  
600 Single-Diode and Two-Diode Solar Cell Parameters by Using a Chaotic Optimization  
601 Approach, *Energies*. 12 (2019). doi:10.3390/en12214209.
- 602 [14] K. Yu, B. Qu, C. Yue, S. Ge, X. Chen, J. Liang, A performance-guided JAYA  
603 algorithm for parameters identification of photovoltaic cell and module, *Appl. Energy*.  
604 237 (2019) 241–257. doi:10.1016/j.apenergy.2019.01.008.
- 605 [15] P.J. Gnetchejo, S. Ndjakomo Essiane, P. Ele, R. Wamkeue, D. Mbadjoun Wapet, S.  
606 Perabi Ngoffe, Important notes on parameter estimation of solar photovoltaic cell,  
607 *Energy Convers. Manag.* 197 (2019) 111870. doi:10.1016/j.enconman.2019.111870.
- 608 [16] X. Chen, K. Yu, Hybridizing cuckoo search algorithm with biogeography-based  
609 optimization for estimating photovoltaic model parameters, *Sol. Energy*. 180 (2019)  
610 192–206. doi:10.1016/j.solener.2019.01.025.
- 611 [17] M. Abd Elaziz, D. Oliva, Parameter estimation of solar cells diode models by an  
612 improved opposition-based whale optimization algorithm, *Energy Convers. Manag.*  
613 171 (2018) 1843–1859. doi:10.1016/j.enconman.2018.05.062.
- 614 [18] M. Merchaoui, A. Sakly, M.F. Mimouni, Particle swarm optimisation with adaptive  
615 mutation strategy for photovoltaic solar cell/module parameter extraction, *Energy*  
616 *Convers. Manag.* 175 (2018) 151–163. doi:10.1016/j.enconman.2018.08.081.
- 617 [19] A.M. Beigi, A. Maroosi, Parameter identification for solar cells and module using a  
618 Hybrid Firefly and Pattern Search Algorithms, *Sol. Energy*. 171 (2018) 435–446.  
619 doi:10.1016/j.solener.2018.06.092.
- 620 [20] X. Gao, Y. Cui, J. Hu, G. Xu, Z. Wang, J. Qu, H. Wang, Parameter extraction of solar  
621 cell models using improved shuffled complex evolution algorithm, *Energy Convers.*  
622 *Manag.* 157 (2018) 460–479. doi:10.1016/j.enconman.2017.12.033.
- 623 [21] X. Chen, B. Xu, C. Mei, Y. Ding, K. Li, Teaching–learning–based artificial bee colony  
624 for solar photovoltaic parameter estimation, *Appl. Energy*. 212 (2018) 1578–1588.  
625 doi:10.1016/j.apenergy.2017.12.115.

- 626 [22] M. Louzazni, A. Khouya, K. Amechnoue, A. Gandelli, M. Mussetta, A. Craciunescu,  
627 Metaheuristic algorithm for photovoltaic parameters: Comparative study and prediction  
628 with a Firefly algorithm, *Appl. Sci.* (2018). doi:10.3390/app8030339.
- 629 [23] D. Kler, P. Sharma, A. Banerjee, K.P.S. Rana, V. Kumar, PV cell and module efficient  
630 parameters estimation using Evaporation Rate based Water Cycle Algorithm, *Swarm*  
631 *Evol. Comput.* (2017). doi:10.1016/j.swevo.2017.02.005.
- 632 [24] P. Lin, S. Cheng, W. Yeh, Z. Chen, L. Wu, Parameters extraction of solar cell models  
633 using a modified simplified swarm optimization algorithm, *Sol. Energy.* 144 (2017)  
634 594–603. doi:10.1016/j.solener.2017.01.064.
- 635 [25] J.P. Ram, T.S. Babu, T. Dragicevic, N. Rajasekar, A new hybrid bee pollinator flower  
636 pollination algorithm for solar PV parameter estimation, *Energy Convers. Manag.* 135  
637 (2017) 463–476. doi:10.1016/j.enconman.2016.12.082.
- 638 [26] A. Fathy, H. Rezk, Parameter estimation of photovoltaic system using imperialist  
639 competitive algorithm, *Renew. Energy.* 111 (2017) 307–320.  
640 doi:10.1016/j.renene.2017.04.014.
- 641 [27] M. Derick, C. Rani, M. Rajesh, M.E. Farrag, Y. Wang, K. Busawon, An improved  
642 optimization technique for estimation of solar photovoltaic parameters, *Sol. Energy.*  
643 157 (2017) 116–124. doi:10.1016/j.solener.2017.08.006.
- 644 [28] D. Oliva, M. Abd El Aziz, A. Ella Hassanien, Parameter estimation of photovoltaic  
645 cells using an improved chaotic whale optimization algorithm, *Appl. Energy.* (2017).  
646 doi:10.1016/j.apenergy.2017.05.029.
- 647 [29] K. Yu, J.J. Liang, B.Y. Qu, X. Chen, H. Wang, Parameters identification of  
648 photovoltaic models using an improved JAYA optimization algorithm, *Energy*  
649 *Convers. Manag.* 150 (2017) 742–753. doi:10.1016/j.enconman.2017.08.063.
- 650 [30] X. Chen, K. Yu, W. Du, W. Zhao, G. Liu, Parameters identification of solar cell  
651 models using generalized oppositional teaching learning based optimization, *Energy.*  
652 99 (2016) 170–180. doi:10.1016/j.energy.2016.01.052.
- 653 [31] L. Guo, Z. Meng, Y. Sun, L. Wang, Parameter identification and sensitivity analysis  
654 of solar cell models with cat swarm optimization algorithm, *Energy Convers. Manag.*  
655 (2016). doi:10.1016/j.enconman.2015.11.041.
- 656 [32] N.F.A. Hamid, N.A. Rahim, J. Selvaraj, Solar cell parameters identification using  
657 hybrid Nelder-Mead and modified particle swarm optimization, *J. Renew. Sustain.*  
658 *Energy.* 8 (2016) 015502. doi:10.1063/1.4941791.

- 659 [33] Y. Zhang, P. Lin, Z. Chen, S. Cheng, A Population Classification Evolution Algorithm  
660 for the Parameter Extraction of Solar Cell Models, *Int. J. Photoenergy*. (2016).  
661 doi:10.1155/2016/2174573.
- 662 [34] N.T. Tong, W. Pora, A parameter extraction technique exploiting intrinsic properties  
663 of solar cells, *Appl. Energy*. (2016). doi:10.1016/j.apenergy.2016.05.064.
- 664 [35] M. Jamadi, F. Merrikh-Bayat, M. Bigdeli, Very accurate parameter estimation of  
665 single- and double-diode solar cell models using a modified artificial bee colony  
666 algorithm, *Int. J. Energy Environ. Eng.* (2016). doi:10.1007/s40095-015-0198-5.
- 667 [36] E.E. Ali, M.A. El-Hameed, A.A. El-Fergany, M.M. El-Arini, Parameter extraction of  
668 photovoltaic generating units using multi-verse optimizer, *Sustain. Energy Technol.*  
669 *Assessments*. (2016). doi:10.1016/j.seta.2016.08.004.
- 670 [37] C. Chellaswamy, R. Ramesh, Parameter extraction of solar cell models based on  
671 adaptive differential evolution algorithm, *Renew. Energy*. (2016).  
672 doi:10.1016/j.renene.2016.06.024.
- 673 [38] A.R. Jordehi, Time varying acceleration coefficients particle swarm optimisation  
674 (TVACPSO): A new optimisation algorithm for estimating parameters of PV cells and  
675 modules, *Energy Convers. Manag.* (2016). doi:10.1016/j.enconman.2016.09.085.
- 676 [39] J. Ma, K.L. Man, S.-U. Guan, T.O. Ting, P.W.H. Wong, Parameter estimation of  
677 photovoltaic model via parallel particle swarm optimization algorithm, *Int. J. Energy*  
678 *Res.* 40 (2016) 343–352. doi:10.1002/er.3359.
- 679 [40] Z. Chen, L. Wu, P. Lin, Y. Wu, S. Cheng, Parameters identification of photovoltaic  
680 models using hybrid adaptive Nelder-Mead simplex algorithm based on eagle strategy,  
681 *Appl. Energy*. 182 (2016) 47–57. doi:10.1016/j.apenergy.2016.08.083.
- 682 [41] X. Yuan, Y. He, L. Liu, Parameter extraction of solar cell models using chaotic asexual  
683 reproduction optimization, *Neural Comput. Appl.* 26 (2015) 1227–1239.  
684 doi:10.1007/s00521-014-1795-6.
- 685 [42] L.H.I. Lim, Z. Ye, J. Ye, D. Yang, H. Du, A linear identification of diode models from  
686 single I-V characteristics of PV panels, *IEEE Trans. Ind. Electron.* 62 (2015) 4181–  
687 4193. doi:10.1109/TIE.2015.2390193.
- 688 [43] A. El-Fergany, Efficient Tool to Characterize Photovoltaic Generating Systems Using  
689 Mine Blast Algorithm, *Electr. Power Components Syst.* 43 (2015) 890–901.  
690 doi:10.1080/15325008.2015.1014579.

- 691 [44] D.F. Alam, D.A. Yousri, M.B. Eteiba, Flower Pollination Algorithm based solar PV  
692 parameter estimation, *Energy Convers. Manag.* 101 (2015) 410–422.  
693 doi:10.1016/j.enconman.2015.05.074.
- 694 [45] F. Dkhichi, B. Oukarfi, A. Fakkar, N. Belbounaguia, Parameter identification of solar  
695 cell model using Levenberg–Marquardt algorithm combined with simulated annealing,  
696 *Sol. Energy.* 110 (2014) 781–788. doi:10.1016/j.solener.2014.09.033.
- 697 [46] Q. Niu, L. Zhang, K. Li, A biogeography-based optimization algorithm with mutation  
698 strategies for model parameter estimation of solar and fuel cells, *Energy Convers.*  
699 *Manag.* (2014). doi:10.1016/j.enconman.2014.06.026.
- 700 [47] Q. Niu, H. Zhang, K. Li, An improved TLBO with elite strategy for parameters  
701 identification of PEM fuel cell and solar cell models, *Int. J. Hydrogen Energy.* (2014).  
702 doi:10.1016/j.ijhydene.2013.12.110.
- 703 [48] D. Oliva, E. Cuevas, G. Pajares, Parameter identification of solar cells using artificial  
704 bee colony optimization, *Energy.* (2014). doi:10.1016/j.energy.2014.05.011.
- 705 [49] A. Laudani, F. Riganti Fulginei, A. Salvini, High performing extraction procedure for  
706 the one-diode model of a photovoltaic panel from experimental I–V curves by using  
707 reduced forms, *Sol. Energy.* 103 (2014) 316–326. doi:10.1016/j.solener.2014.02.014.
- 708 [50] X. Yuan, Y. Xiang, Y. He, Parameter extraction of solar cell models using mutative-  
709 scale parallel chaos optimization algorithm, *Sol. Energy.* 108 (2014) 238–251.  
710 doi:10.1016/j.solener.2014.07.013.
- 711 [51] S.J. Patel, A.K. Panchal, V. Kheraj, Extraction of solar cell parameters from a single  
712 current–voltage characteristic using teaching learning based optimization algorithm,  
713 *Appl. Energy.* 119 (2014) 384–393. doi:10.1016/j.apenergy.2014.01.027.
- 714 [52] A. Askarzadeh, A. Rezaadeh, Extraction of maximum power point in solar cells using  
715 bird mating optimizer-based parameters identification approach, *Sol. Energy.* (2013).  
716 doi:10.1016/j.solener.2013.01.010.
- 717 [53] A. Askarzadeh, A. Rezaadeh, Artificial bee swarm optimization algorithm for  
718 parameters identification of solar cell models, *Appl. Energy.* (2013).  
719 doi:10.1016/j.apenergy.2012.09.052.
- 720 [54] L.L. Jiang, D.L. Maskell, J.C. Patra, Parameter estimation of solar cells and modules  
721 using an improved adaptive differential evolution algorithm, *Appl. Energy.* 112 (2013)  
722 185–193. doi:10.1016/j.apenergy.2013.06.004.

- 723 [55] O. Hachana, K.E. Hemsas, G.M. Tina, C. Ventura, Comparison of different  
724 metaheuristic algorithms for parameter identification of photovoltaic cell/module, *J.*  
725 *Renew. Sustain. Energy.* (2013). doi:10.1063/1.4822054.
- 726 [56] A. Askarzadeh, A. Rezazadeh, Parameter identification for solar cell models using  
727 harmony search-based algorithms, *Sol. Energy.* (2012).  
728 doi:10.1016/j.solener.2012.08.018.
- 729 [57] W. Gong, Z. Cai, Parameter extraction of solar cell models using repaired adaptive  
730 differential evolution, *Sol. Energy.* 94 (2013) 209–220.  
731 doi:10.1016/j.solener.2013.05.007.
- 732 [58] M.F. AlHajri, K.M. El-Naggar, M.R. AlRashidi, A.K. Al-Othman, Optimal extraction  
733 of solar cell parameters using pattern search, *Renew. Energy.* (2012).  
734 doi:10.1016/j.renene.2012.01.082.
- 735 [59] K.M. El-Naggar, M.R. AlRashidi, M.F. AlHajri, A.K. Al-Othman, Simulated  
736 Annealing algorithm for photovoltaic parameters identification, *Sol. Energy.* 86 (2012)  
737 266–274. doi:10.1016/j.solener.2011.09.032.
- 738 [60] M.R. AlRashidi, M.F. AlHajri, K.M. El-Naggar, A.K. Al-Othman, A new estimation  
739 approach for determining the I–V characteristics of solar cells, *Sol. Energy.* 85 (2011)  
740 1543–1550. doi:10.1016/j.solener.2011.04.013.
- 741 [61] M. Ye, X. Wang, Y. Xu, Parameter extraction of solar cells using particle swarm  
742 optimization, *J. Appl. Phys.* (2009). doi:10.1063/1.3122082.
- 743 [62] D. Yousri, M.A. Elaziz, A. Razaee, M. Merchaoui, K.P.S. Rana, T.S. Babu, D. Oliva,  
744 P. Ram, N. Rajasekar, D.F. Alam, M.B. Eteiba, D. Kler, Y. Goswami, V. Kumar,  
745 Comment on “Important notes on parameter estimation of solar photovoltaic cell”, by  
746 Gnetchejo et al. [*Energy Conversion and Management*,  
747 <https://doi.org/10.1016/j.enconman.2019.111870>], *Energy Convers. Manag.* 201  
748 (2019) 112131. doi:10.1016/j.enconman.2019.112131.
- 749 [63] P.J. Gnetchejo, S. Ndjakomo Essiane, P. Ele, R. Wamkeue, D. Mbadjoun Wapet, S.  
750 Perabi Ngoffe, Reply to comment on “Important notes on parameter estimation of solar  
751 photovoltaic cell”, by Gnetchejo et al. [*Energy Conversion and Management*,  
752 <https://doi.org/10.1016/j.enconman.2019.111870>], *Energy Convers. Manag.* (2019).  
753 doi:10.1016/j.enconman.2019.112132.
- 754 [64] D. Yousri, M.A. Elaziz, M. Merchaoui, K.P.S. Rana, T.S. Babu, D. Oliva, P. Ram, N.  
755 Rajasekar, D.F. Alama, M.B. Eteiba, D. Kler, Y. Goswami, V. Kumar, Reply on “Reply  
756 to comment on Important notes on parameter estimation of solar photovoltaic cell”, by

- 757 Gnetchejo et al. [Energy Conversion and Management, [https://doi.org/10.1016/](https://doi.org/10.1016/j.enconman.2019.111870)  
758 [j.enconman.2019.111870](https://doi.org/10.1016/j.enconman.2019.111870)], Energy Convers. Manag. (2019).  
759 [doi:10.1016/j.enconman.2019.112234](https://doi.org/10.1016/j.enconman.2019.112234).
- 760 [65] D. Veberič, Lambert W function for applications in physics, Comput. Phys. Commun.  
761 183 (2012) 2622–2628. [doi:10.1016/j.cpc.2012.07.008](https://doi.org/10.1016/j.cpc.2012.07.008).
- 762 [66] M.P. Calasan, Analytical solution for no-load induction machine speed calculation  
763 during direct start-up, Int. Trans. Electr. Energy Syst. 29 (2019) e2777.  
764 [doi:10.1002/etep.2777](https://doi.org/10.1002/etep.2777).
- 765 [67] R.M. Corless, G.H. Gonnet, D.E.G. Hare, D.J. Jeffrey, D.E. Knuth, On the LambertW  
766 function, Adv. Comput. Math. 5 (1996) 329–359. [doi:10.1007/BF02124750](https://doi.org/10.1007/BF02124750).
- 767 [68] M. Calasan, A. Nedic, Experimental Testing and Analytical Solution by Means of  
768 Lambert W-Function of Inductor Air Gap Length, Electr. Power Components Syst.  
769 (2018). [doi:10.1080/15325008.2018.1488012](https://doi.org/10.1080/15325008.2018.1488012).
- 770 [69] S.M. Perovich, M. Orlandic, M. Calasan, Concerning exact analytical STFT solutions  
771 to some families of inverse problems in engineering material theory, Appl. Math.  
772 Model. (2013). [doi:10.1016/j.apm.2012.10.052](https://doi.org/10.1016/j.apm.2012.10.052).
- 773 [70] S.M. Perovich, M.P. Calasan, R. Toskovic, On the exact analytical solution of some  
774 families of equilibrium critical thickness transcendental equations, AIP Adv. 4 (2014)  
775 117124. [doi:10.1063/1.4902161](https://doi.org/10.1063/1.4902161).
- 776 [71] S.M. Perovich, M.D. Djukanovic, T. Dlabac, D. Nikolic, M.P. Calasan, Concerning a  
777 novel mathematical approach to the solar cell junction ideality factor estimation, Appl.  
778 Math. Model. 39 (2015) 3248–3264. [doi:10.1016/j.apm.2014.11.026](https://doi.org/10.1016/j.apm.2014.11.026).
- 779 [72] S.M. Perovich, M. Calasan, D. Kovac, I. Tosic, Concerning an analytical solution of  
780 some families of Kepler's transcendental equation, AIP Adv. (2016).  
781 [doi:10.1063/1.4944836](https://doi.org/10.1063/1.4944836).
- 782 [73] M.P. Calasan, An invertible dependence of the speed and time of the induction  
783 machine during no-load direct start-up, Automatika. 61 (2020) 141–149.  
784 [doi:10.1080/00051144.2019.1689725](https://doi.org/10.1080/00051144.2019.1689725).
- 785 [74] A.F. Zobaa, S.H.E.A. Aleem, A.Y. Abdelaziz, Classical and Recent Aspects of Power  
786 System Optimization, Academic Press, 2018. [doi:10.1016/C2016-0-03379-X](https://doi.org/10.1016/C2016-0-03379-X).
- 787 [75] M. Kumar, A. Kumar, An efficient parameters extraction technique of photovoltaic  
788 models for performance assessment, Sol. Energy. 158 (2017) 192–206.  
789 [doi:10.1016/j.solener.2017.09.046](https://doi.org/10.1016/j.solener.2017.09.046).



- 790 [76] M.G. Villalva, J.R. Gazoli, E.R. Filho, Comprehensive Approach to Modeling and  
791 Simulation of Photovoltaic Arrays, *IEEE Trans. Power Electron.* 24 (2009) 1198–1208.  
792 doi:10.1109/TPEL.2009.2013862.
- 793 [77] E.A. Silva, F. Bradaschia, M.C. Cavalcanti, A.J. Nascimento, Parameter Estimation  
794 Method to Improve the Accuracy of Photovoltaic Electrical Model, *IEEE J.*  
795 *Photovoltaics.* 6 (2016) 278–285. doi:10.1109/JPHOTOV.2015.2483369.
- 796 [78] S. Bana, R.P. Saini, A mathematical modeling framework to evaluate the performance  
797 of single diode and double diode based SPV systems, *Energy Reports.* 2 (2016) 171–  
798 187. doi:10.1016/j.egy.2016.06.004.
- 799 [79] R. Szabo, A. Gontean, Photovoltaic Cell and Module I-V Characteristic  
800 Approximation Using Bézier Curves, *Appl. Sci.* 8 (2018) 655.  
801 doi:10.3390/app8050655.
- 802 [80] E. Salahshour, M. Malekzadeh, R. Gholipour, S. Khorashadizadeh, Designing multi-  
803 layer quantum neural network controller for chaos control of rod-type plasma torch  
804 system using improved particle swarm optimization, *Evol. Syst.* 10 (2019) 317–331.  
805 doi:10.1007/s12530-018-9222-3.
- 806 [81] E. Salahshour, M. Malekzadeh, F. Gordillo, J. Ghasemi, Quantum neural network-  
807 based intelligent controller design for CSTR using modified particle swarm  
808 optimization algorithm, *Trans. Inst. Meas. Control.* 41 (2019) 392–404.  
809 doi:10.1177/0142331218764566.
- 810 [82] M. B. M. Rozlan, A. F. Zobaa, S. H. E. Abdel Aleem, The optimisation of stand-alone  
811 hybrid renewable energy systems using HOMER, *Int. Rev. Electr. Eng.* 6 (2011) 1802–  
812 1810.
- 813 [83] M. Malekzadeh, A. Khosravi, M. Tavan, An immersion and invariance based input  
814 voltage and resistive load observer for DC–DC boost converter, *SN Appl. Sci.* 2 (2020)  
815 78. doi:10.1007/s42452-019-1880-7.